12-20-2012

Condition-Dependent Risk Assessment of Large-Scale Grid-Tied Photovoltaic Power Systems

Sherwin Li
University of Connecticut - Storrs, sherwin.li@engr.uconn.edu

Condition-Dependent Risk Assessment of Large-Scale Grid-Tied Photovoltaic Power Systems

Sherwin Li

B.S., the Pennsylvania State University, 2009

A Thesis

Submitted in Partial Fulfillment of the

Requirements for the Degree of

Master of Science

At the

University of Connecticut

2012

APPROVAL PAGE

Masters of Science Thesis

Condition-Dependent Risk Assessment of Large-Scale Grid-Tied Photovoltaic Power Systems

Presented by

Sherwin Li, B.S.

Major Advisor_____
Peng Zhang

Associate Advisor_____
Peter Luh

Associate Advisor_____
Yaakov Bar-Shalom

Associate Advisor_____
Sheng-li Zhou

University of Connecticut

2012

Abstract

Condition-Dependent Risk Assessment of Large-Scale Grid-Tied Photovoltaic Power Systems

Sherwin Li, M.S. Electrical Engineering

The University of Connecticut, 2012

Major Advisor: Peng Zhang

This thesis reviews the methods for evaluating the reliability of large PV systems and techniques for quantifying the impacts of PV interconnection on distribution system reliability. In addition, a comparative study is performed to evaluate the seasonal condition-dependent risk performance of central-inverter and string-inverter grid-tied PV power systems. Major contributions include: 1) risk analysis of seasonal impacts for string and centralized PV systems. Seasonal sensitivities of PV system risks to system structures, temperature variation, solar insolation, and capacitor equivalent series resistance are analyzed; and 2) the incorporation of the effect of operational conditions and the aging failure model into the PV system risk analysis. The PV panel aging effect, over a time span of 25 years, is incorporated to the reliability model. The risk performance is then analyzed with respect to the number of PV strings, PV panel failure rate and inverter repair time. The effectiveness of the proposed method has been validated on two real-life 20kW grid-connected PV systems. Application of the proposed method to actual large PV systems can provide valuable information to manage PV system risks, to choose better PV system design options, to develop better maintenance strategies, and thus to realize maximum benefit of photovoltaic power. Finally, future research trend for the emerging Giga-PV power systems is identified and discussed.

Acknowledgments

I would like to convey my gratitude to my research adviser, Prof. Peng Zhang, for his guidance and continuous support that have made this thesis possible. I am honored to be his first graduate student to graduate. I am proud to be a member of his Power and Energy Systems Laboratory.

Sincere thanks to Prof. Peter Luh, Prof. Yaakov Bar-Shalom and Prof. Shengli Zhou for sharing their valuable insights and advices for my thesis. Special thanks to my colleagues, Ali Abdollahi and Dr. Yang Wang for their supports and mentorships.

I would also like to thank my grandmother. You may be gone but will never be forgotten. Our shared memories are engrained in my heart forever.

Finally, my deepest gratitude goes to my beloved parents and my sister for their continuous encouragements and prayer supports.

Table of Contents

List of Figures

List of Tables

Publications

1. A. Abdollahi, P. Zhang, H. Xue, and **S. Li**, "Enhanced Subspace-Least Mean Square for fast and accurate power system measurement," *IEEE Trans. Power Delivery*, vol. 28, no. 1, pp. 383-393, Jan. 2013.
2. P. Zhang, W. Li, **S. Li**, Y. Wang, "Reliability assessment of photovoltaic power systems: Review of current status and future perspectives," *Applied Energy*, Accepted for publication.
3. **S. Li**, P. Zhang, A. Abdollahi, Y. Wang, and W. Li, "Condition-dependent risk assessment of large grid-tied photovoltaic power systems," to be submitted to *IEEE Trans. Power Systems.*

Chapter 1 INTRODUCTION

Electricity generated from photovoltaic (PV) power systems is a major renewable energy source which involves zero greenhouse gas emission and no fossil fuel consumption. The total capacity of grid-connected PV power systems has been grown exponentially from 300 MW in 2000 to about 67 GW in 2011 [1]. This capacity, however, is not firm because of the unreliable nature and probabilistic behavior of PV power systems.

Relatively high risks exist both inside and outside of PV power systems [2]. First, a PV power system is composed of many vulnerable components whose lifecycle reliability is highly susceptible to temperature, power losses, and ambient environments. Meanwhile, solar insolation and power input of PV system are highly variable and uncontrollable; leading to high electrical stress in PV panels that may shorten the operational lifecycles and power electronic interfaces and consequently results in a lower system reliability compared to conventional generation plants. Second, high penetration of PV generation will bring detrimental effect to power distribution network. Significant reverse power flow may cause unacceptable voltage rise on distribution feeder. Overvoltage may trigger the protection in PV inverters, which as a result will shut down PV generation, causing sudden change in power flow and abrupt voltage fluctuation. Reverse power flow and voltage fluctuation may also increase the number of operations of on-load tap changers (OLTCs), which will shorten the useful lives of transformers. Distribution networks connected with PVs, therefore, have a high risk for increased maintenance costs and

power outages, which necessitate methodologies and tools to quantify the reliability of grid-connected PV systems.

The purposes of PV reliability analysis is to evaluate PV system performance and to generate reliability indices that is helpful in selecting the best design option at the planning stage, and is useful in determining measures to reduce cost and increase benefit at the operational stage. Risk assessment is of fundamental importance for planning and operation of both PV power systems and PV-connected distribution networks. Its major utilities include:

1) Quantifying risks in PV systems and choosing optimal PV system design
2) Determining effective measures to mitigate risks
3) Justifying acceptable PV penetration level in distribution network
4) Probabilistically evaluating the impacts of intermittent PV resources on power system adequacy, security, spinning reserve, planning and real-time operation
5) Designing reconfigurable distributed energy storage to leverage PV application
6) Finding planning and operational solutions to address the challenges of high penetration of PV to distribution network in a least cost manner while achieving the maximum level of reliability.

Risk assessment of PV power systems, therefore, is an indispensable technology that assures reliable PV generation integration. Practical applications of PV risk assessment theory will bring direct and indirect benefits for both utility companies and customers including increased revenue, higher energy yield, improved power quality, extended equipment operational life and less carbon emission.

A large PV system is normally tied to power grid [3], which not only eliminates the need for expensive and short-lived batteries but also takes advantage of grid power supply and voltage support. Central inverter structure and string inverter configuration are two mainstream topologies [4] of grid-connected PV power systems. The former is known for its arguably lower cost of a central inverter, while the latter for its arguably higher energy yields. So far, however, there is still a lack of systematic, comparative investigation into the risk performance of the two topologies. This is partly due to the complex nature of PV power system topology [5-7]. Nonetheless, the most difficult factor is that the reliability and failure modes of PV power system components are highly dependent on their operational conditions such as temperature [2], power losses [8, 9], electrical stresses [10-12], and ambient environments [13, 14].

This research develops a comprehensive framework for comparative analysis of risks in the two types of grid-connected PV power systems. First, the impact of seasonal time-varying input-power levels and ambient conditions on the failure rates of critical components such as PV modules, inverters and capacitors are incorporated in the PV risk analysis. Second, aging failures of PV panels are formulated in the risk assessment. A state enumeration method is adopted to analyze real-life central inverter and string inverter topologies. Several risk metrics are proposed to quantify PV system risk and its impact on PV system operation and energy output. Sensitivity analyses are extensively conducted to compare the performances of centralized topology with those of multiple-string topology, which serves a useful guide for factorial design of grid-tied PV systems.

Chapter 2 LITERATURE REVIEW

Increasing attention is being paid to PV system reliability in recent years due to rapid growth of PV power installation in residential and commercial buildings as well as military bases. Cost-reduction in production of PV modules together with economic incentives offered by government will further increase the installed capacity of solar power in the foreseeable future. Failures in PV systems, therefore, will result in significant amount of economic losses [15]. The reliability of grid-connected PV power systems has been of great concern to both utility companies and customers [16].

Although the PV reliability issue was already identified three decades ago [17], reliability quantification of an entire PV generation station remains unresolved due to the complex nature of PV systems. The existing literature mostly focuses on reliability assessment for the power electronic components such as IGBT [9], capacitor [18] and inverter [10], [19], whereas much fewer references discuss the reliability evaluation for entire PV system. References [6, 7] presented simplified, system-level models for PV system reliability using a Markov modeling concept. Hierarchical reliability block diagram was developed [12] to model the behavior of PV system. Reference [13] quantified the impact of inverter failures on total lifetime of PV system using Monte Carlo simulation. Reference [20] proposed Latin Hypercube Sampling (LHS) technique to integrate stratified and random sampling in order to improve its computational speed for obtaining the reliability indices. In the above literature, failure rates of electronic elements in a PV system are treated as constants. These parameters, however, actually vary with system states including solar insolation [21], ambient temperature [14], and

load level [22]. The unrealistic assumptions in reliability analysis may give inaccurate or misleading results. For instance, it was concluded that “capacitors’ contribution to failure rate is “quite small” [23], which seems against industrial practice.

On the topic of grid integration of PVs, the National Renewable Energy Laboratory (NREL) has conducted extensive surveys to explore the impact of high penetration PVs on power system planning and operation [24]. It has been identified that PV integration is closely tied to overall distribution system reliability [25]. Recently, a framework, which based on Markov reward models (MRM), is proposed to integrate reliability and performance analysis of grid-tied PV systems [26]. This proposed framework may help understanding the trade-offs between repair policies and replacement/overhaul costs. In addition, the effect of reactive power shortage on the distribution network with high PV penetration has been studied [27]. Hence, it is obvious that reliability assessment theory suitable for distribution systems integrated with PV generation has become a highly needed technology to build a high-penetration renewable energy future. In the era of smart grid, the microgrid is a mainstream solution for grid integration of PV systems. Reliability evaluation of active distribution systems including PV microgrids becomes a major technical challenge to be tackled.

In previous work, the microgrid was often treated as a small sized conventional power grid where the failure modes of power electronic interfaces were not considered in microgrid reliability evaluation [28-32]. These methods may be practical for estimating microgrids with combined heat and power plants (CHPs) or conventional generators, but are not suitable to analyze distribution network with PVs or other renewable sources. The effect of converter topologies is incorporated into reliability evaluation of DC microgrid

by the use of minimum cut sets [33]. This approach, however, neither considered the impact of power losses and ambient condition on converter reliability nor can be extended to distribution system reliability assessment. Reference [34] has pointed out that modeling the operation mode transitions is a major challenge in reliability evaluation of microgrids. Reliability of PV/wind microgrid operating in an islanded mode was studied using Monte Carlo simulation [35]. Again, this approach only dealt with input power of PV array without considering the reliability of PV inverters. Fault tree analysis (FTA) has been used to evaluate the reliability of islanded microgrid in emergency mode [36]. The limitation is that this FTA approach can only compute small-scale systems and cannot deal with interconnected modes. It has been realized that a multi-state model is needed for modeling PV generators due to the intermittent nature of solar radiation [37]. This method, however, neither considered the impact of input power and temperature on system reliability nor modeled islanded modes of PV microgrids. An analytical approach was proposed [38] to study the effect of distributed generators (DG) on distribution reliability, where the DG outputs, DG failures and load variations were considered. An event-based Monte Carlo method was developed [39] to evaluate the effect of intentional islanding and switching operations on distribution reliability. Furthermore, pseudo-sequential Monte Carlos has been adopted for the reliability of the active distribution networks [40]. The former approach is unable to deal with flexible operation modes of microgrids, and the latter assume constant loads and DG outputs under islanding situations without considering the intermittent features of DGs.

In summary, the following technical issues remain unresolved or are still under further investigation:

1) Developing power-input/power-loss/temperature-dependent failure rates for power electronic components in PV systems;
2) Incorporating a power input curve and PV voltage regulation schemes into PV reliability assessment;
3) Defining PV reliability metrics to quantify energy availability and outage time;
4) Building the multi-state model of PV microgrid by using reliability results of PV systems;
5) Developing new reliability evaluation algorithms to evaluate active distribution systems with embedded PV microgrids.

The following section offers a systematic and detailed summary of PV reliability evaluation technologies recently developed. Practical approaches to quantification of the effect of input power and ambient conditions on the failure rates of critical PV components are introduced. An effective state enumeration method to analyze real-life PV array configurations is presented. Reliability indices are discussed as useful guidelines for PV system design, operation and maintenance. We also describe a non-sequential simulation method for reliability evaluation of active distribution system with multiple embedded PV microgrids.

2.1 **Reliability evaluation of grid-connected PV systems**

Large-scale grid-connected PV systems are usually connected either in a centralized or a string/multi-string structure, as shown in Figs. 1 and 2 respectively. The distinguishing feature of the string inverter system is that each string has its own inverter to convert DC electricity to AC output. If a centralized system has the same total capacity as an n-string-inverter system, the capacity of each string inverter is only one-nth of that of the central

inverter. Another PV topology is the micro-inverter system [41, 42]. In this structure, the micro-inverter and the PV panel are integrated as one electrical device, which is directly connected to distribution grid through an AC bus, as shown in **Figure 2.3.** The purpose of the micro-inverter system is to achieve high modularity, easy installation and enhanced safety. In addition, the maximum power point (MPP) of each module can be tracked individually by the corresponding inverter. Hence, this topology has a potential to better optimize the PV power generation under partial shading conditions, compared to the other topologies. On the other hand, micro-inverter system may also improve reliability by reducing converter temperature and eliminating electrolytic capacitors.

As shown in Figure 2.1-3, a PV system consists of *n* PV strings. Each string is responsible for one-*n*th power output of the entire PV system that means the failure of some PV strings will not lead to the failure of the whole PV system, on the contrary only decrease the PV output. This is the key idea in the reliability evaluation of PV system. Note that, in the most methods below, it is assumed that each PV string has the same failure rate and repair rate.

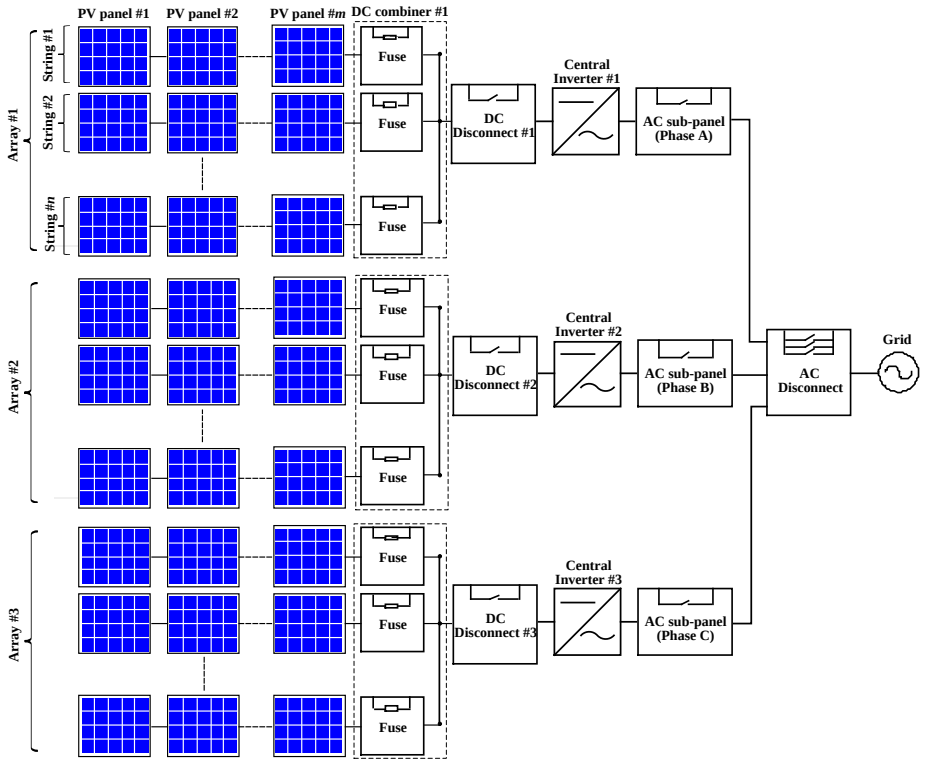

Figure 2.1 Schematic of a central inverter PV system

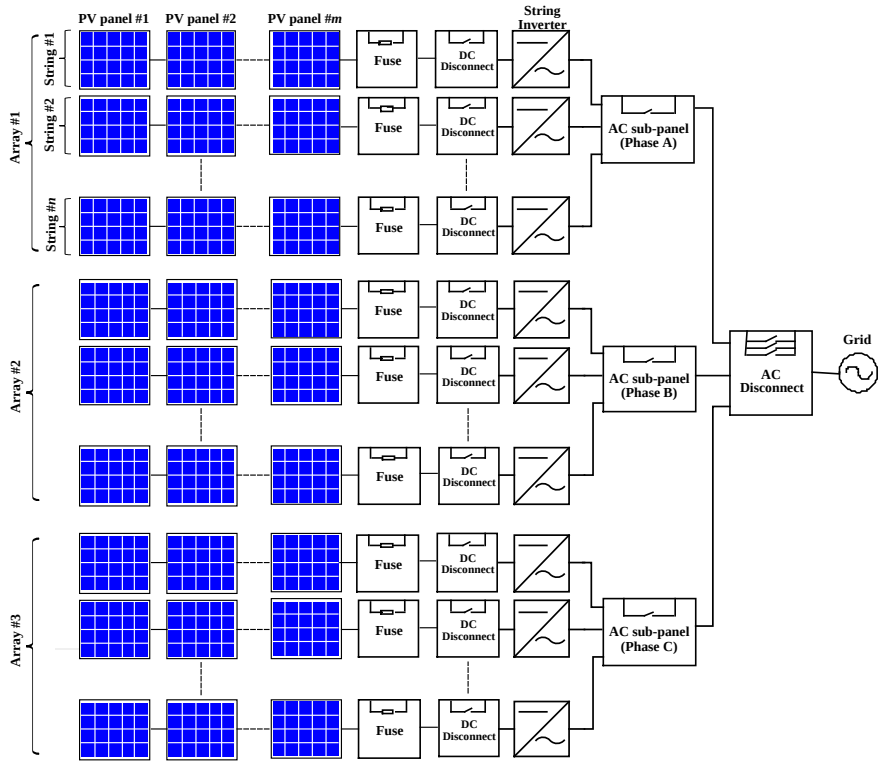

Figure 2.2 Schematic of a string inverter PV system

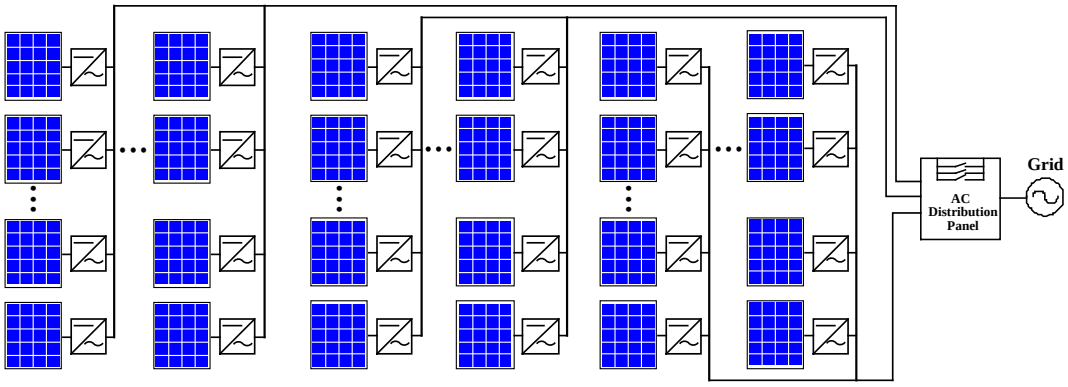

Figure 2.3 Schematic diagram of a micro-inverter PV power system

2.1.1 PV Panels

PV panels are the packaged, connected assembly of PV cells, which are often considered as the most reliable elements in PV systems. Nevertheless, the panels can also fail or degrade in their long-term lifecycle [43, 44]. In the past years, therefore, there were many researches primarily focusing on the reliability of PV panels. In [13], various degradation and failure modes of PV panels are presented. The paper also develops a procedure to assess the degradation, failure modes, as well as their effect on PV panel parameters. Ref. [45] proposed to characterize the degradation effect in terms of maximum power point (MPP) and lost hours due to dust accumulation. However, more experimental results are necessary to validate this idea. Using probability methods, Ref. [8] proposes a mathematical degradation model for reliability predication of PV panels. The model is based on the assumption of linear degradation of reliability parameters and Gaussian distribution of PV power outputs.

Panel topology is another important aspect associated with PV panel reliability. The researches on the topology of PV panels can be traced back to 1980s and even earlier [46, 47]. Recently, the network reliability theories are used to explore reliability of large-scale PV panels. For example, the cut-set technique is used in [48] to investigate the reliability

of several different connection modes of PV panels, i.e., the series, parallel, series-parallel, total-cross-tied, bridge-linked, and their different combinations. This technique, which is based on probability theory, can be applied to calculate the reliability indices of a complex network by reducing it into subsets of system components which are known as cut sets. In order to cause a system failure, all components of a minimal cut set must fail. For reliability analysis, the minimal cut sets are identified and combined in series and the failure probabilities of components are connected in parallel. Then, the concept of union may be applied to the series-connected minimal cut sets to calculate the system reliability. By applying cut-set technique, it was found that total cross-tied (TCT) and bridge-linked (BL) configurations increase the operational lifetime of the PV arrays by 30%.

2.1.2 Inverter

Figure 2.4 Centralized PV inverter (Photo Courtesy: SMA Solar Technology)

Figure 2.5 Microinverter (Photo Courtesy: SMA Solar Technology)

As made by semiconductor modules, inverters are among the vulnerable components in PV systems [17]. A centralized inverter and a microinverter are shown in Figure 2.4 and Figure 2.5, respectively. They are the connection of the switching components, for instance, IGBTs, diodes and capacitors. The reliability of PV inverter depends on the performance of each component in PV inverter. In particular, in grid-connected PV systems, a PV inverter may handle a high level of power flow and operate under high temperature environment, which degrades the inverter reliability and increases the risk of component aging failures. Ref. [49] investigates different circuit topologies of the single-phase PV inverters. Results indicate that failures often occur in switching stage and temperature is the most likely cause of failure.

2.2 **Failure Rates of Power Electronic Switches**

The empirical formula of calculating the failure rate of IGBT (see Figure 2.6) and MOSFET can be found in [50] and [51] respectively. It is observed that the failure rates of IGBT and MOSFET are largely determined by thermal overstress. That means the failure rates of switches are related to power losses and system power input levels since the failure rate is the functions of voltage or temperature while the temperature depends on the power loss that in turn relies on system power input levels. Meanwhile, the empirical formula of the failure rate of diode is given in Refs. [52] and [53]. As diodes are affiliated to IGBT and MOSFET in the same case, the reliability of diodes is also dependent on power losses and system power input levels through temperature and voltage.

Figure 2.6 IGBT Module for high-voltage, high-current PV System (Photo Courtesy: Infineon Technologies)

2.2.1 Thermal Model of IGBT and Diode

A typical single-phase inverter consists of a connection of IGBTs and diodes. A series of empirical formula have been proposed for estimating power losses in IGBTs and diodes as shown in Figure 2.7. Given the power losses, the temperature rise in IGBT and diode can be calculated by the following linear heat transfer equations [53]:

$$\Delta T_{IGBT} = \theta_{11} P_{IGBT\_loss} + \theta_{12} P_{Diode\_loss} \quad (1)$$

$$\Delta T_{Diode} = \theta_{21} P_{IGBT\_loss} + \theta_{22} P_{Diode\_loss} \quad (2)$$

where P_{IGBT_loss} and P_{Diode_loss} are power dissipations in IGBT and diode, respectively. Coefficients θ_{11} and θ_{22} are thermal resistance of IGBT and diode, respectively, while θ_{12} and θ_{21} are thermal coupling coefficients between IGBT and diode.

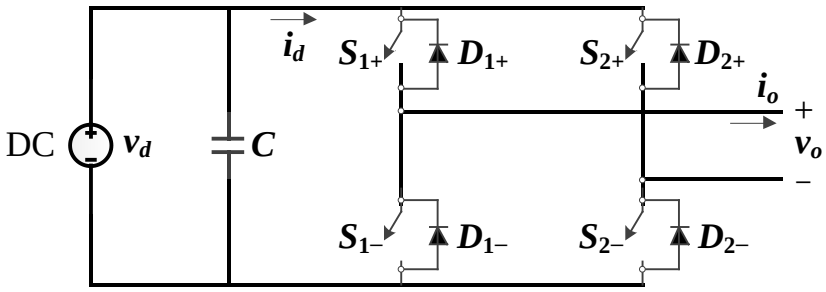

Figure 2.7 Single-phase full-bridge inverter topology

The junction temperatures of IGBT or diode can be calculated by using the following formula

$$T_j = T_c + \Delta T = T_a + \theta_a (P_{IGBT\_loss} + P_{diode\_loss} + P_{add}) + \Delta T \quad (3)$$

where T_a and T_c are the ambient temperature and the case temperature, respectively, θ_a is the thermal resistance from ambient to case including the sink, and P_{add} is the power dissipated by other mounted devices in addition to IGBT and diode.

2.2.2 Failure Rates of IGBT

An empirical formula recommended by FIDES Guide 2009 can be used to estimate the failure rate of IGBT [50], as follows.

$$\lambda_{IGBT} = (\lambda_{0TH}\Pi_{Thermal} + \lambda_{0TCyCase}\Pi_{TCyCase} + \lambda_{0TCySJ}\Pi_{TCySJ} + \lambda_{0RH}\Pi_{RH} + \lambda_{0Mech}\Pi_{Mech})\Pi_{Induced}\Pi_{PM}\Pi_{Process} \quad (4)$$

where λ_{0TH} is the basic failure rate of IGBT due to thermal overstress, $\lambda_{0TCyCase}$ to thermal cycling effect on case, λ_{0TCySJ} to thermal cycling effect on solder joint, λ_{0RH} to humidity, and λ_{0RH} to mechanical overstress. Correspondingly, $\Pi_{Thermal}$, $\Pi_{TCyCase}$, Π_{TCySJ}, Π_{RH}, and Π_{Mech} are the acceleration factors relating to physical overstresses of electrical, thermal, and mechanical origin. $\Pi_{Induced}$ represents the contribution of overstresses cause by other factors, Π_{PM} represents the quality of manufactured parts, and $\Pi_{Process}$ represents the quality and technical control over reliability in the product life cycle.

Given the junction temperature information, the temperature factor is calculated by

$$\Pi_{Thermal} = \Pi_{EI} \cdot e^{11604\times0.7\times[1/293-1/(T_j+273)]} \quad (5)$$

where T_j is junction temperature of IGBT, and

$$\Pi_{EI} = \begin{cases} \left(V_{applied}/V_{r,IGBT}\right)^{2.4} & if \quad \left(V_{applied}/V_{r,IGBT}\right) > 0.3 \\ 0.056 & if \quad \left(V_{applied}/V_{r,IGBT}\right) \le 0.3 \end{cases} \quad (6)$$

Here $V_{applied}$ is the applied voltage across IGBT, and $V_{r,\,IGBT}$ is the rated reverse voltage of IGBT.

It can be seen that the failure rates of IGBTs are related to power loss and system power input levels since the factors are the functions of voltage or temperature while the temperature depends on the power loss that in turn relies on system power input levels.

2.2.3 Failure Rates of Diode

A standard reliability model for diode [54] is adopted to estimate the failure rate of diode in PV inverters, as follows.

$$\lambda_D = \lambda_b \pi_T \pi_S \pi_C \pi_Q \pi_E \tag{7}$$

where λ_b is the base failure rate of diode, π_T is the temperature factor, π_S is the electrical stress factor, π_C is the construction factor, π_Q and π_E are the quality and environment factor, respectively. Give the junction temperature T_j, the temperature factor is calculated by

$$\pi_T = e^{-3091\left(1/(T_j+273)-1/298\right)} \tag{8}$$

The electrical stress factor [55] can be calculated by

$$\pi_S = \begin{cases} \left(V_{applied}/V_{r,diode}\right)^{2.45} & if \quad 0.3 < V_{applied}/V_{r,diode} < 1 \\ 0.054 & if \quad V_{applied}/V_{r,diode} \le 0.3 \end{cases} \tag{9}$$

where $V_{applied}$ is the applied voltage across diode, and $V_{r,\,diode}$ is the rated reverse voltage of diode..

Similar to the IGBT, the failure rates of diode are related to power loss and system power input levels through temperature and voltage.

2.2.4 Failure Rates of Capacitor

Capacitor failure is another major factor leading to the failure of inverter. Ref. [56] compares six different PV module-integrated inverters. The results show that the electrolytic capacitor is the dominant component for inverter failure, not the MOSFET. Moreover, “PV industry representatives at the DOE workshop agreed that the most urgent problem affecting inverter reliability is the quality of the dc-bus capacitors” [57].

Classical method to predict reliability of electrolytic capacitors can be found in MIL-HDBK-217, in which the failure rate of a capacitor is dependent on the applied DC voltage, ripple current and ambient conditions (temperature, airflow, heat sinking). In particular, PV systems mounted outdoor may suffer from a relatively high failure rate of capacitors due to the harsher ambient environment. The failure rate of capacitor is, therefore, mainly determined by the core temperature, which can be calculated by the base life at elevated maximum core temperature and the actual core temperature [58]. This failure rate formula is derived from the Arrhenius's law [59], and in agreement with the "life doubles every 10 ºC" rule for capacitors.

A commonly accepted formula [53] is adopted to compute the failure rate of capacitor, as expressed by

$$\lambda_C = \frac{1}{r_C} = \frac{1}{L_b \cdot 2^{(T_{\max} - T_c)/10}} \tag{10}$$

where r_C is the life expectancy of capacitor, L_b is the base life at elevated maximum core temperature T_{max} such as 95 ℃, T_c is the actual core temperature. Equation (10) is in agreement with the "life doubles every 10 ºC" rule for capacitors, which can be derived from the Arrhenius's law.

Equation (10) shows that life time estimation for capacitor is a function of core temperature, which mainly depends on the ripple current flowing through the capacitor. Given a centralized inverter system without storage component, the current ripple can be approximately calculated as below:

$$i_r(t) = \frac{V_o}{V_d} I_o \cos(2\omega t - \varphi) \tag{11}$$

where V_o and I_o represents the RMS values of grid voltage and output current, V_d is the DC input voltage, ω is the fundamental frequency, and φ is the power factor. Note that higher order harmonics produced by on/off switching are neglected here due to much smaller amplitudes [54].

From (11), the RMS ripple current is

$$I_r = \frac{P_o}{\sqrt{2} V_d} \tag{12}$$

where P_o is the output power of inverter.

The core temperature of capacitor in steady-state [52], therefore, can be calculate by

$$T_c = T_a + \theta_c (I_r^2 R_s) \tag{13}$$

where R_s is the equivalent series resistance of capacitor, θ_c is the thermal resistance from capacitor core to environment, and T_a is the ambient temperature.

Substituting (13) into (10) yields the power loss related failure rate of capacitor.

2.3 **Inverter Topologies**

Beside component reliability analysis for inverters, some papers aim at the various structures of inverters. For instance, the reliability of a single-stage three-phase integrated inverter is investigated in [60], where the thermal behavior is integrated into the reliability model of PV system. In [23], the reliability of more inverter configurations is studied, including an integrated topology, a two-stage configuration, and a three-stage

one. Different connections between the modules and inverters, i.e., the AC-bus level and DC-bus level connections are explored in [41]. Results show that higher system reliability can be achieved by using module-integrated inverters. Moreover, a systematic approach to studying the reliability of power-electronic components in a PV inverter can be found in [15], and Ref. [61] even presents a coherent methodology for integrating reliability considerations into the design of fault-tolerant power electronic systems. Moreover, Ref. [62] proposed an optimal design methodology for transformerless PV inverters. It calculates the optimal configuration of components by minimizing the levelized cost of electricity (LCOE) which takes into consideration of the failure rate of components. This optimal design methodology may help lower the manufacturing and maintenance costs of the PV converters.

2.4 **Inverter Reliability**

In general, a PV inverter has no parallel redundancy, meaning a failure in any one component will lead to an outage of the entire inverter. Therefore, the reliability of PV inverter can be modeled as a series network. The failure rate, repair time and availability of the PV inverter are expressed by

$$\lambda_I(P,V,T) = \lambda_C + \sum_i (\lambda_{Di} + \lambda_{Si}) \tag{14}$$

$$r_I(P,V,T) = \frac{1}{\lambda_I}\left[\lambda_C r_C + \sum_i (\lambda_{Di} r_{Di} + \lambda_{Si} r_{Si})\right] \tag{15}$$

$$A_I(P,V,T) = \frac{1/r_I}{\lambda_I + 1/r_I} \tag{16}$$

where λ_I is the failure rate, r_I is the repair time, A_I is the availability, the subscripts *S*, *D* and *C* represents IGBT, diode and capacitor, respectively, and *i* denotes the *i*th

component. As noted in (14)-(16), all three indices are functions of power flow through the PV inverter, input voltage and temperature.

In addition, the availabilities of DC disconnect and AC subpanel can be computed from their failure rates and repair times, as follows

$$A_{DC} = \frac{1/r_{DC}}{\lambda_{DC} + 1/r_{DC}} \tag{17}$$

$$A_{AC} = \frac{1/r_{AC}}{\lambda_{AC} + 1/r_{AC}} \tag{18}$$

The three-phase AC disconnect can be assumed to be perfectly reliable since it is normally closed with very low failure possibility. It can be easily modeled if its failure data is available.

2.5 **Reliability evaluation techniques for PV systems**

2.5.1 Markov Process Method

The stochastic behavior of a PV system can be viewed as a Markov process and described by Markov space state diagram. The transitions between various Markov states are due to failures and repairs of PV strings/modules/inverters. By solving the state transition matrix, the steady states of the Markov model can be obtained. The primary outputs of the Markov model are the steady-state probabilities and the operating time in each state. Based on Markov method, the economic costs of component failure are calculated in [63] by introducing cost rates to each state and cost impulses to the transitions of the Markov chain. The Markovian framework proposed in [64] provides performance-related metrics (e.g. energy yield) on top of the traditional reliability models (e.g. MTBF). However, Markov chain suffers the curse of dimensionality and restricts its

application to low-dimensional spaces. Additionally, this method did not address the intermittent nature of the solar input. Thus, more research is required to reformulate the reward vector to introduce input uncertainty to the PV energy yield estimation. Meanwhile, Markov state space diagrams are drawn in [6] and [65] for reliability evaluation of the central-inverter PV system and distributed-inverter PV system.

2.5.2 Monte-Carlo Simulation

As an often-used method, *Monte-Carlo* simulation is also used in reliability analysis of PV systems [15], [12] and [66]. For highly complex system, Monte-Carlo simulation is preferred because its computational efficiency is independent from either the size or the complexity of the system. Thus, *Monte-Carlo* simulation owns much more flexibility and can be able to study more complicated problems, such as reliability assessment of PV-Wind hybrid system in [67]. There are two types of Monte-Carlo (MC) simulation: sequential MC and non-sequential MC. Sequential MC calculates the states based on the transitional probabilities and the correlations between the chronologically-sampled random variables can be included [68, 69]. It is used to quantify the reliability indices of microgrid consists of wind and PV generation. Results show that this type of microgrid is more unreliable than the ones with conventional generation [70]. On the other hand, non-sequential MC calculates the states based on their probability distributions [71]. By comparison, sequential MC often requires longer time to reach convergence than non-sequential MC. Psuedo-chronological MC simulation was proposed to retain the efficiency of non-sequential MC and to model chronological loads in sequential MC [72]. This method was demonstrated on IEEE-MRTS (Modified Reliability Test System) [73],

results show that it took the same computational time compared to the non-sequential MC, with much better accuracy of the chronological load patterns.

2.5.3 State Enumeration

State Enumeration Method (SEM) is used in [74] and [75] to compute the reliability indices of PV system. This method accounts for the impacts of power inputs, voltage levels and power losses on the failure rates of the panel components; hence, on the PV array as a whole. The assumption is that each PV string has two mutually exclusive states: the working state and the out-of-service state. First, the equivalent reliability parameters for all the PV strings in a PV array are computed. Then, using SEM, can be applied to determine the reliability indices of the PV array. There are two types of indices: time-oriented and energy-oriented. More details about these indices are included in the next section. As a generic and flexible method, SEM is applicable to any structures such as centralized-/string-/micro- inverter structure, and also to both the homogenous and heterogeneous PV strings.

2.5.4 Reliability Block Diagram

Using Reliability Block Diagram (RBD), Ref. [7] develops the Photovoltaic Reliability and Performance Model (PV-RPM). The combined model can predict PV system energy output when taking into account the availability of components, solar irradiance, and module and inverter performance. PV-RPM consists of three components: Failure modes and effects analysis (FMEA), accelerated life tests and system reliability/availability modeling. FMEA helps systematically identifying, analyzing and documenting all the possible failure scenarios and their impacts on the rest of the system. Accelerated life test

runs the components, such as PV panels, under elevated stress to collect the time-to-failure data. System reliability/availability model is a diagram that represents all the subsystem and component events that must occur for a successful system operation. Recently, failure modes effects and criticality analysis (FMECA) for PV system is proposed to provide a thorough understanding of the system failure modes [76]. The criticality of FMECA is a quantitative index scale that represents the seriousness of the failure modes. This enables priority ranking among all the failure modes and their impacts on the system. However, FMECA is an inductive analysis method which requires a profound and detailed knowledge about every single component failure modes of the system.

2.5.5 Fault Tree Analysis

Fault Tree Analysis (FTA) was first developed in 1961 by the US Air Force. It translates a physical system into a structured logic diagram, known as fault trees. It not only considers the basic events that cause failures, but also represents the relationships of ambient condition and human error in causing failures. In general, FTA consists of four basic steps [77]:

1. System definition
2. Fault-tree construction
3. Qualitative evaluation
4. Quantitative evaluation

Although FTA is a powerful tool for reliability assessment, it requires a high cost of development for first-time application to a system. Nevertheless, as the system

complexity grows and with potentially catastrophic failure consequences, FTA method remains as the preferred tool in reliability assessment.

Ref. [78] analyzes simple stand-alone PV systems using the Failure Mode Effect Analysis (FMEA) and FTA. Three typical solar photovoltaic systems are discussed in this paper. In [4], a method based on FTA is proposed for assessing the reliability of large-scale grid-connected photovoltaic systems. In [17], FTA and Markov process method are used to describe the behavior of PV system. The life-cycle energy cost of PV system is calculated and applied to PV system designs.

Chapter 3 RESEARCH WORK

3.1 Risk Modeling of PV Components and Systems

Large grid-connected PV systems are usually connected either in a centralized or a string/multi-string structure as shown in Figures 1-2. The distinguished feature of the string inverter system is that each string has its own inverter to convert DC electricity to AC. If a centralized system has the same total capacity as an *n*-string-inverter system, the capacity of each string inverter is only one-*n*th of that of the central inverter.

A systematic approach is adopted for the risk evaluation of PV systems, as illustrated in Figure 3.1. The flowchart can be explained as follows.

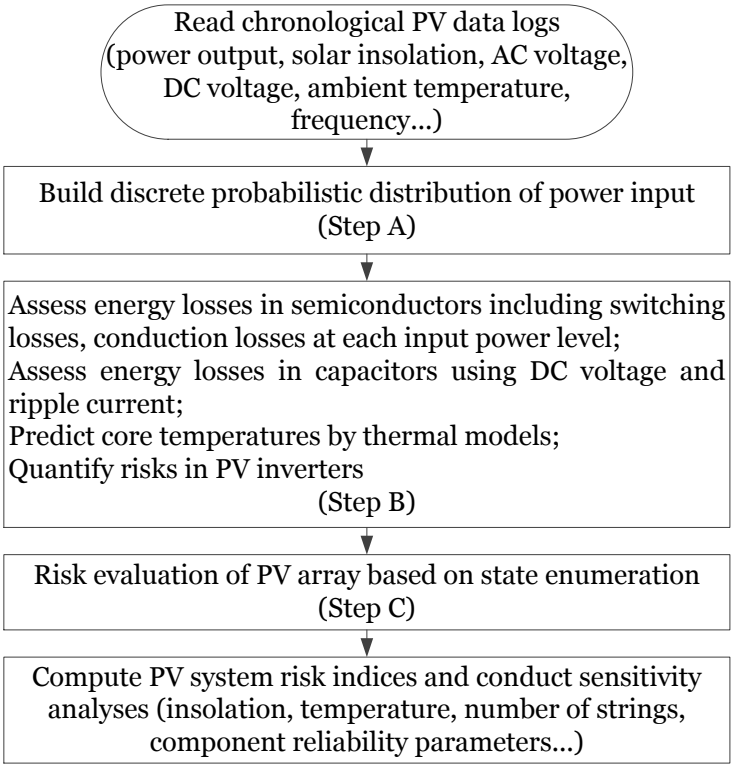

Figure 3.1 Flowchart of PV risk analysis

3.1.1 Seasonal Discrete Probability Distribution of Input Power

Fluctuating seasonal input power of PV system causes varying energy losses in power

electronic switches and capacitors, resulting in temperature variations in PV inverter components. Therefore, input power level is a critical factor in determination of life cycle risks in PV inverter and PV system. In real-life, data logger of PV system normally samples and records system variables every 1-15 minutes, which produces a chronological, highly intermittent power curve containing a large amount of data points. For the sake of seasonal-based risk analysis, the input power curve is divided into four seasons, as illustrated in Figure 3.2(a). In order to quantify their contribution to operational risks in PV systems, the input power measurements can be aggregated into a discrete probability distribution. *K*-means clustering technique is introduced to eliminate the chronology and to cluster data points into several power-level groups. The procedures are presented as follows.

First, assume the annual power curve is to be divided in to *K* power levels. The value of *K* is adjustable, depending on the level of detail required for reliability analysis. For real-life PV systems, our experiments show that *K* can be set between 10-15, which guarantees satisfactory results depending on cases.

Then, an annual power curve with *N* data points can be clustered into *K* power levels in the following steps.

(i) Prepare initial clusters $\boldsymbol{S}=\{\boldsymbol{S}_1, \boldsymbol{S}_2, \ldots, \boldsymbol{S}_K\}$ by arbitrarily assigning data points to each cluster; calculate initial cluster mean μ_i, where *i* corresponds to cluster $\boldsymbol{S}_i$, $i = 1, 2, \ldots, K$.

(ii) Calculate the distance d_{ji} from each data point P_j ($j = 1, 2, \ldots, N$) to the *i*th cluster mean μ_i, i.e.,

$$d_{ji} = | P_j - \mu_i | \tag{19}$$

(iii) Assign each data point P_j to the nearest cluster with minimum distance for j = 1, 2, … , N; re-calculate cluster means by

$$\mu_i = \frac{1}{N_{S_i}} \sum_{P_j \in S_i} P_j, \qquad i = 1, 2, \cdots, K \tag{20}$$

where N_{S_i} is the number of data points in the ith cluster.

(iv) Repeat steps (ii) and (iii) until each and every μ_i remains unchanged between two iterations.

(v) The converged μ_i is the ith mean power level with the discrete probability p_i equaling to N_{S_i} / N where N is the number of power curve considered. If the time window is a year and sampling interval is 10 *min*, N=8760×6=52560.

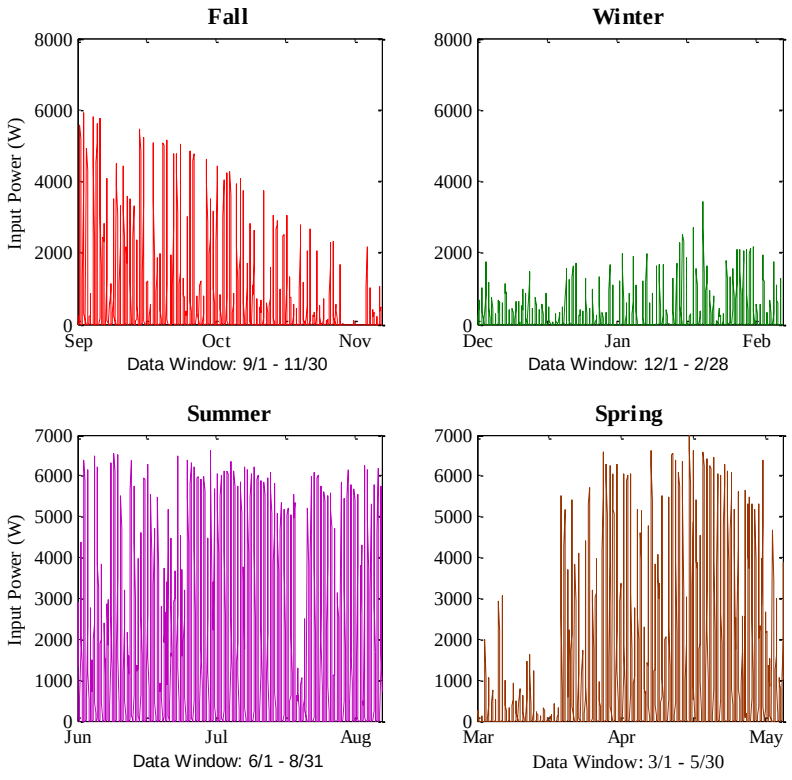

(a)

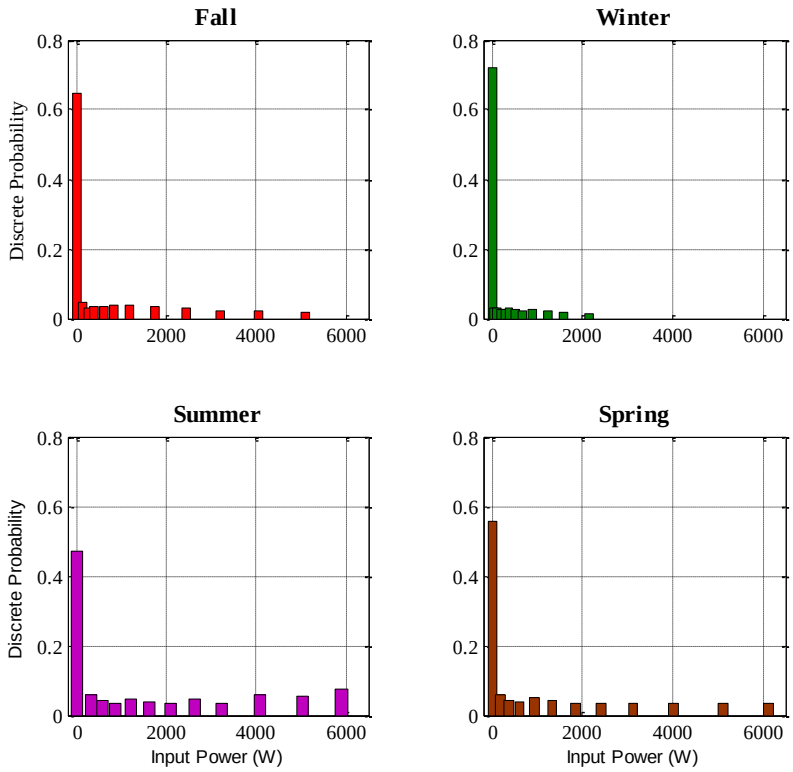

(b)

Figure 3.2 Power input of phase A inverter for four seasons (a) Chronological seasonal power curve (b) Discrete probability distribution of power input

For instance, aggregating the seasonal power curve in Figure 3.2(a) into 12 power levels through *K*-means method generates a corresponding discrete probability distribution, as shown in Figure 3.2(b). Each power level in the discrete probability distribution is used to evaluate the availabilities of power electronic components at that power level and the expected seasonal energy output and other risk indices are weighted by the probability of each power level.

3.2 **Reliability Evaluation of PV Array**

3.2.1 Equivalent Reliability Parameters of PV String

A PV string is a serial connection of PV panels and a fuse inside a dc combiner. There are two repairable failure modes for PV panels that result in loss of the whole

string: failure at a junction box and short-circuit of PV panel. Both result in outage of a whole PV string until the failure is cleaned. These two failure modes are characterized by an average failure rate and an average repair rate of PV panel. A PV panel may also be bypassed by diodes due to an open failure or shading effect. The bypass of PV panel generally could lower the output of a string, rather than causing an outage of the string. In this paper, we do not consider the bypass of panels in the series formula because this effect is not an outage and has been represented in the input power levels. Moreover, the probability of simultaneous bypass of multiple modules is extremely low, which is negligible. The equivalent reliability parameters of a PV string can be calculated by

$$\lambda_S = \sum_{i=1}^{m} \lambda_{P,i} + \lambda_F \tag{21}$$

$$r_S = \frac{1}{\lambda_S}\left(\sum_{i=1}^{m} \lambda_{P,i} r_{P,i} + \lambda_F r_F \right) \tag{22}$$

where λ and r represent the failure rate and repair time, respectively, m is the number of PV panels in a PV string. Here the subscripts S, P, F indicate the equivalent PV string, PV panel, and the fuse in the DC combiner, respectively, $\lambda_{P,i}$ is the failure rate of the ith PV panel, and $r_{P,i}$ is the repair time for the ith PV panel.

3.2.2 State Enumeration of Reliability Analysis of PV Array

Once the reliability parameters for all n PV strings in a PV array are obtained, a state enumeration method can be developed to compute reliability parameters of the array. State enumeration is a generic method which is applicable to both homogenous and heterogeneous PV strings.

In general, all possible states of a PV array can be expanded from the following logic expression

$$(A_{S1}+U_{S1})(A_{S2}+U_{S2})\cdots(A_{S,n}+U_{S,n}) \tag{23}$$

where n is the number of PV strings in a PV array, $A_{S,i}$ and $U_{S,i}$ are the availability and unavailability of the ith PV string, respectively, and can be calculated as follows:

$$A_{Si}=\frac{1/r_{Si}}{\lambda_{Si}+1/r_{Si}} \tag{24}$$

$$U_{Si}=\frac{\lambda_{Si}}{\lambda_{Si}+1/r_{Si}} \tag{25}$$

where λ_{Si} and r_{Si} are calculated using (21)-(22).

The probability of an enumerated state α of the PV array is given by

$$p_A(\alpha)=\prod_{i=1}^{n_f}U_{Si}\prod_{i=1}^{n-n_f}A_{Si} \tag{26}$$

where n_f and $n-n_f$ are the numbers of failed and non-failed PV strings in state α.

All enumerated states in which j PV strings fails are aggregated into the jth state of the PV array. The probability of the jth state is then expressed by

$$p_{Aj}=\sum_{\alpha\in G(n_f=j)}p_A(\alpha)=\sum_{\alpha\in G(n_f=j)}\left(\prod_{i=1}^{n_f}U_{Si}\prod_{i=1}^{n-n_f}A_{Si}\right)\quad j=0,\cdots,n \tag{27}$$

In (27), $G(n_f=j)$ denotes the set of enumerated states corresponding to a total of j strings out of service. In particular, States 0 is the full-up state where all n strings in an array operate properly. State 1 corresponds to the derated state with one PV string out of

service ($n-1$ contingency), State j to the $n-j$ contingency where j-out-of- n PV strings are down ($n-j$ contingency), and State n to the outage of all n PV strings. In addition, a full-down state is often due to common causes such as lightning, hail, fire, and other electrical or mechanical problems, but not due to independent failures of n strings. The common cause failure can be easily incorporated into the enumeration process as an additional failure event.

It should be noted that the main purpose of this section is to provide one viable approach to incorporate impacts of system power inputs, voltage levels and power losses on failure rates of components and in turn on the reliability of whole PV arrays.

3.2.3 Aging and Degradation Effects in PV Risk Analysis

The chance of PV panel failure will significantly increase with advancing age. The power output from PV panel also degrades over time. Both factors should be considered in performing risk analysis whenever a PV module gets into the end stage of life. In this paper, a linear model is adopted to model PV panel degradation [54] i.e. the power output of PV array decreases over years as follows

$$p_i = p_0[1-(k-1)d] \qquad k = 1,\ldots,L \tag{28}$$

where p_0 is the initial power capacity of a PV module, d is the constant slope, k represents a specified service year, L is the observed life cycle.

A practical aging failure model is adopted to calculate the annual unavailability due to aging failure, as briefly summarized below.

Given a failure density probability function $f(t)$ for aging failure, the probability of transition to aging failure of a PV string in a subsequent period t after having survived for T years can be calculated by

$$P_{T,t} = \frac{\int_T^{T+t} f(t)dt}{\int_T^{\infty} f(t)dt} \tag{29}$$

By dividing t into N small intervals with the same length Δx, the failure probabilities in the ith interval can be calculated by

$$P_i = \frac{\int_T^{T+i\Delta x} f(t)dt - \int_T^{T+(i-1)\Delta x} f(t)dt}{\int_T^{\infty} f(t)dt} \quad (i=1,2,\ldots,N) \tag{30}$$

If a failure happened in the ith interval, the corresponding average unavailability duration can be estimated by

$$UD_i = t - (2i-1)\Delta x/2 \quad (i=1,2,\ldots,N) \tag{31}$$

The unavailability in a specified subsequent t period can be calculated by

$$U_{T,t} = \sum_{i=1}^{N} P_i \cdot UD_i / t \tag{32}$$

where t is often one year period.

Finally, for a PV string considering both repairable and non-reparable aging failures, its total unavailability and availability in a subsequent period t after having survived for T years can be estimated by

$$U_S = U_{S,r} + U_{T,t} - U_{S,r}U_{T,t} \tag{33}$$

$$A_S = 1 - U_S \tag{34}$$

where A_S and U_S are the total availability and unavailability of PV string, respectively.

3.3 PV System Risk Indices

Besides commonly used risk indices such as failure rate and outage duration, two new risk indices are introduced: energy-oriented and time-oriented indices. The proposed indices can be used to quantify PV system performance and are therefore useful in selecting the best design option at the planning stage and in determining measures to reduce cost and increase benefit at the operational stage.

3.3.1 Energy-Oriented Indices

The energy-oriented indices provide annual statistics of PV project yields considering system uncertainties.

3.3.1.1 *Ideal Output Energy (IOE)*

IOE is the power generated from a perfectly reliable PV system, which can be estimated by multiplying clustered power levels by the corresponding converter efficiency curve, as follows

$$IOE = \sum_{l} \sum_{i=1}^{K} \mu_i \eta_i p_i D \tag{35}$$

where K is the number of input power levels for a single phase, and the subscript i and l denote the ith input power level and lth phase, respectively. μ_i is the mean of the ith input power level, η_i is the efficiency of PV inverter at μ_i, p_i is the probability of the ith power level, and D is the total time length considered. If the annual IOE is considered, then D = 8760 hours. Note that the subscript l denoting lth phase in each variable in previous equations has been omitted for simplicity. Unless specifically noted, the subscript l for lth phase is always omitted in this paper. Note that IOE is the ideal energy output of a PV

system in the first year of its life cycle as a reference when considering PV degradation and aging failure for different service ages.

3.3.1.2 *Expected Output Energy (EOE)*

With non-perfect reliability, the expected power output of PV system is the ideal output multiplying the system availability. Numerically, the sum of the expected output at each power level multiplied by the probability of each power level gives the total expected output energy.

For *central inverter system*, the expected energy is estimated by

$$EOE = \sum_{l} \left[\sum_{i=1}^{K} \eta_i p_i D \sum_{j \in \{0,1,2,\cdots,n-1\}} f_j \mu_i p_{Aj} A_{I,ij}(f_j \mu_i, V_{DC,i}) \right] A_{DC} A_{AC} \tag{36}$$

where p_{Aj} is the probability of jth State of the PV array, A_{Iij} is the availability of the inverter at the ith input power level and jth State of the PV array, $f_j\mu_i$ represents the expected input power of inverter considering PV array failures, and A_{DC} and A_{AC} denote the availabilities of the DC disconnect and AC sub-panel, respectively. f_j is a ratio that takes the value 1 for State 0, $(n-1)/n$ for State 1, $(n-2)/n$ for State 2, and $(n-j)/n$ for State j, if the PV array is composed of n homogeneous strings. Obviously, A_{Iij} is a function of input power $f_j\mu_i$ and inverter DC side voltage $V_{DC,i}$.

For *string inverter PV system*, the expect energy is estimated by a different formula:

$$EOE = \sum_{l} \left[\sum_{i=1}^{K} \eta_i p_i D \sum_{j \in \{0,1,2,\cdots,n-1\}} f_j \mu_i p_{Aj}(\mu_{str,i}, V_{DC,str,i}) \right] A_{AC} \tag{37}$$

where $\mu_{str,i}$ is the input power of string inverter at the *i*th power level, and $V_{DC,\mathrm{str},i}$ is the DC side voltage of string inverter. p_{Aj} is a function of power flow through the string inverters and the DC side voltage. Other symbols are the same as defined in (36).

The major difference between (36) and (37) is that the failure risk in string inverter has been implicitly incorporated in state probability p_{Aj} in (37).

3.3.1.3 *Energy Availability (A_e)*

The A_e is defined as normalized *EOE* on the basis of *IOE*.

$$A_e = \frac{EOE}{IOE} \tag{38}$$

Note that *IOE* is a constant corresponding to the ideal energy in the first year.

3.3.2 Time-Oriented Indices

The time-oriented indices are introduced to quantify the annual outage time and annual available time of PV power systems. Those indices are useful for justifying maintenance requirements for PV systems.

3.3.2.1 *Time Availability (A_t)*

A_t is a relative measure of how many hours the PV power system is expected to operate in normal conditions every year.

For *central inverter system* with multiple phases,

$$A_t = \prod_l \left[\sum_{i=1}^{K} p_i \, p_{A0} A_{I,i0}(f_0 \mu_i, V_{DC,i}) A_{DC} A_{AC} \right] \tag{39}$$

For *string inverter system* with multiple phases,

$$A_t = \prod_l \left[\sum_{i=1}^{K} p_i \, p_{A0}(\mu_{str,i}, V_{DC,str,i}) A_{AC} \right] \tag{40}$$

A_t represents the percentage of time when the whole PV system does not need repair or replacement. Note that the time availability includes the time when the PV system has a zero MW output due to no solar insolation.

The time availability for a single phase can be calculated using the items contained within the bracket in (39) and (40). For simplicity, here the subscript l for lth phase in each variable has been omitted.

The time unavailability is calculated by

$$U_t = 1 - A_t \tag{41}$$

Note that the unavailability includes the probabilities that the PV power system operates in various derated states with parts of PV strings out of service (e.g. $n-1$, $n-2$ conditions, etc.). The probability for single derated state can also be obtained by state enumeration method if necessary.

3.3.2.2 *Available (H_{av}), Derated (H_{dr}) and Outage Hours (H_{dw})*

The fully-available hours H_{av} is calculated by

$$H_{av} = A_t \cdot 8760 \tag{42}$$

H_{dw} represents the average time for whole plant shutdown and is calculated as follows:

For the central inverter system,

$$H_{dw} = 8760 \cdot \prod_l \left[1 - \sum_{i=1}^{K} p_i \sum_{j \in \{0,1,2,\cdots,n-1\}} p_{Aj} A_{I,ij}(f_j \mu_i, V_{DC,i}) A_{DC} A_{AC} \right] \tag{43}$$

For the string inverter system,

$$H_{dw} = 8760 \cdot \prod_{l} \left[1 - \sum_{i=1}^{K} p_i \sum_{j \in \{0,1,2,\cdots,n-1\}} p_{Aj}(\mu_{str,i}, V_{DC,str,i}) A_{AC} \right] \tag{44}$$

The total time of the PV system in derated states is calculated by

$$H_{dr} = 1 - H_{av} - H_{dw} \tag{45}$$

The time-oriented reliability indices help one understand the well-being of PV system and perform intelligent asset management.

Chapter 4 TEST RESULTS

Reliability analyses are performed using a real-life central-inverter PV system connected to BC Hydro distribution network and an alternative design option with string inverter topologies, as shown in Figure 2.1 and Figure 2.2 respectively. Note that, in the test cases, it is not necessary to apply inverter efficiency curve on the power input since the inverter output and DC voltage are directly measured. The reliability parameters of the two systems are summarized in Table A-I in the Appendix, whereas the discrete probability model for annual power outputs of the PV system is given in Tables A-II.

4.1 Reliability Results for Base Case

By using the reliability parameters in Tables A-I, the reliability results for the base case (i.e. reliability indices of PV system for the first year of service), are obtained and listed in Table I.

Table I Reliability indices for Base Cases

Energy Indices	*EOE* (MWh)	*IOE* (MWh)		A_e
Central inverter	20.06	20.265		0.99024
String inverter	20.14	20.265		0.99396
Time Indices	A_t	H_{av} (hrs)	H_{dr} (hrs)	H_{dw} (hrs)
Central inverter	0.90682	7943.74	816.25	0.0095
String inverter	0.90049	7888.29	871.70	0.0059

The results show that the reliability performances of the two systems are very close. The string inverter system is slightly better in terms of energy availability, whereas the central inverter system is slightly advantageous with higher fully-available time. The

rationale behind the results includes:

(i) The failure frequency of the string inverter system is higher because more inverters are installed than those in the central inverter system. Thus the fully-available time is less than that of the central inverter system.

(ii) The outage of a string inverter only impacts itself but the outage of the central inverter impacts all strings. Therefore, the string inverter system has relatively higher energy availability.

4.2 **Effect of PV Degradation and Aging Failure**

To observe the long-term performance of the PV systems with various structures, The A_e and A_t for 25 years are calculated. The results are shown in Figure 4.1.

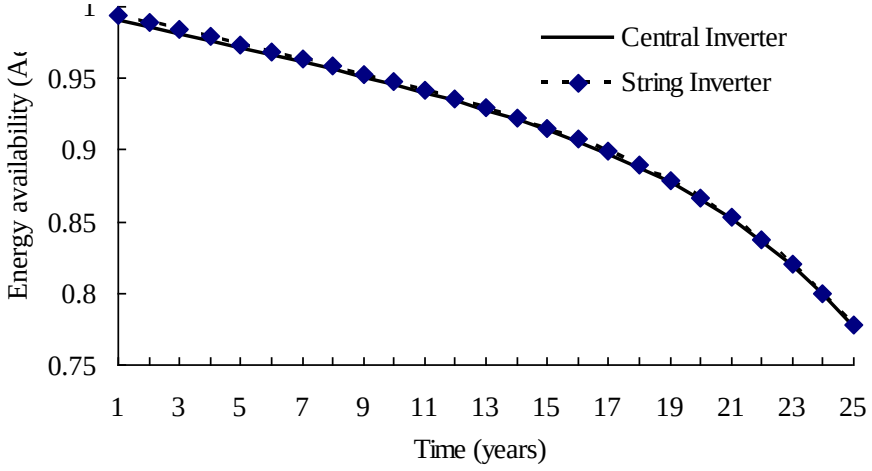

(a) Energy-based availability

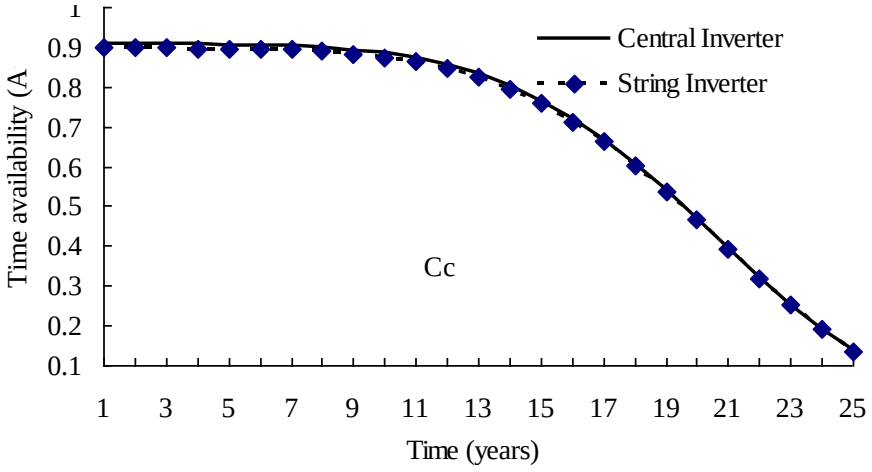

(b) Time-based availability

Figure 4.1 Reliability indices for 25 years with array degradation

The following observations can be made from Figure 4.1:

(1) In both PV systems, A_e and A_t are very sensitive to the change of service age. At the end of life, the values of A_e and A_t are very low, especially for A_t, which indicates a high repair requirement at the end of useful life.

(2) A_t is relatively insensitive to the increase of service age in the first fifteen years, but quickly goes down while approaching to the mean life of PV array. In contrast to A_t, the decreasing trend of A_e is smoother. The phenomenon reveals that A_e can catch the changes of both PV efficiency degradation and aging failure, whereas A_t mainly reflects the influence of aging failure because PV degradation can only has an indirect impact on A_t due to the effect of decreased input power of inverter on component failure rates.

(3) A_e and A_t are very close at the end of life cycle. The phenomenon is due to the fact that the effect aging failure dominates when the PV system approaches to the end of life.

4.3 **Temperature Impact on PV Risk Assessment**

The impact of ambient temperature on PV system risks was explored. A central inverter is presumably located inside an electrical room with cooling facilities, whereas string

inverters are typically mounted outdoor. Thus, in the sensitivity study, the effective ambient temperature for the central inverter is assumed to vary between 0℃ and 40℃, while the ambient temperature for string-inverter varies from 0℃ to 60℃ considering its direct exposure to sunlight and working in high heat emitted by PV panels. Risk analysis results with temperature from 40℃ and 60℃ are also calculated for the central inverter system for the comparison purpose only. The risk analysis results for lower temperature are not listed because the changes in risk performances are not appreciable when the temperature is below 0℃. Figure 4.2 summarizes the sensitivity results.

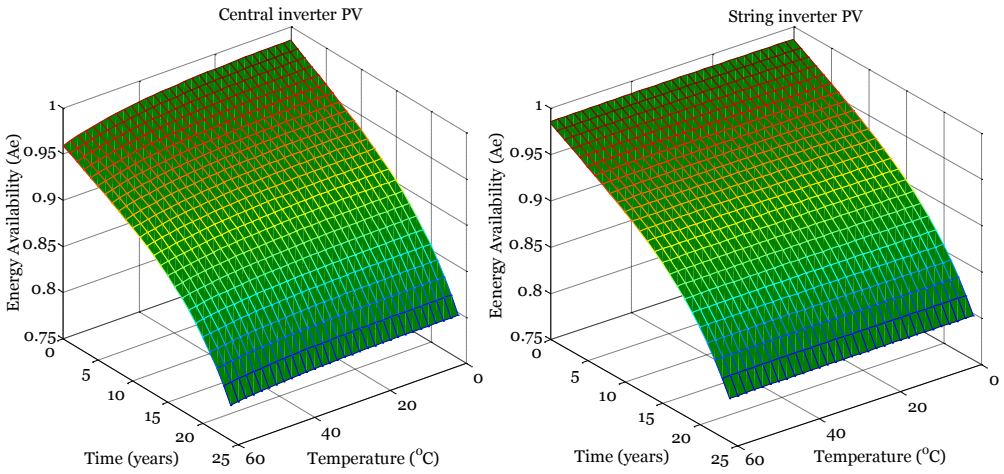

(a) Energy availability (A_e)

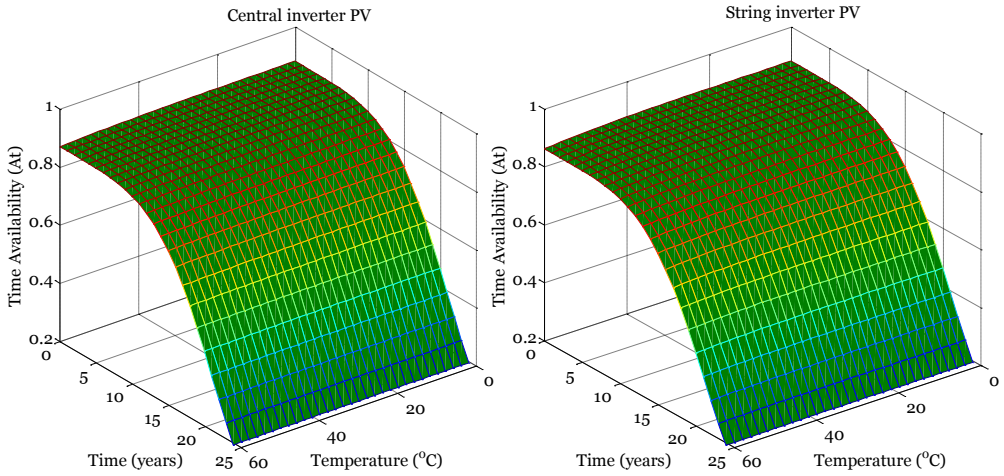

(b) Time availability (A_t)

Figure 4.2 Temperature effect on reliability with degradation

It can be observed from Figure 4.2 that:

(1) The risk level of both types of PV systems is increased with temperature rise. For the first year, A_e decreases from 99.36% to 96.69% in the central inverter PV system when the ambient temperature changes from 0℃ to 60℃. However, in the string inverter, A_e only decreases from 99.44% to 99.26%. This means the string-inverter system is more temperature-tolerant than the central inverter system from an energy availability perspective. A similar conclusion of A_e can be drawn from the results obtained using the data for the 25^{th} year, but it is not as obvious as that for the first year because the aging failure has dominated the failure over the effect of temperature on the PV system.

(2) For the first year, the time availability index A_t also drops with temperature rise from 90.84% to 89.47% in the central inverter system and from 90.83 to 88.68% in the string inverter system. This means that more maintenance activities are required if the effect of temperature is taken into consideration.

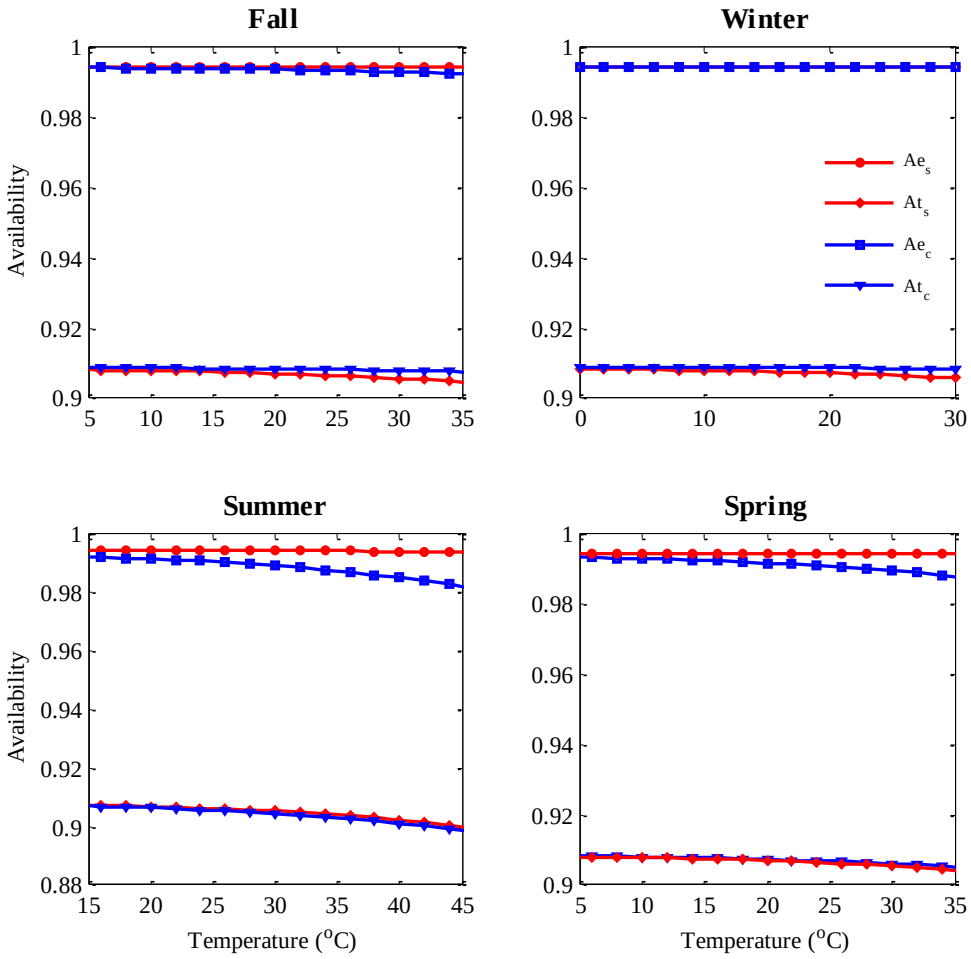

Figure 4.3 Seasonal temperature effect on reliability

The seasonal temperature impact on PV system reliability was explored. In the study shown in Figure 4.3, the ambient temperatures for the inverters are assumed to vary between 5° C and 35°C in fall and spring, 0°C and 30°C in winter and 15° C and 45°C in summer. For each season, an ambient temperature interval of 30°C is considered as shown in Figure 4.3.

It can be observed from Figure 4.3 that string inverter system has a higher A_e and a lower A_t relative to central inverter system in fall, winter and spring. Thus, the seasonal results for fall, winter, and spring are in accordance with the annual base case as shown in Table I which shows string system has better A_e while central system has better A_t.

However, during summer, string system presents both higher A_e and higher A_t than the central system.

Table II Statistical parameters of seasonal energy availability index (temperature sensitivity test)

	mean		Higher mean value	Standard deviation $\times 10^{-3}$		Less sensitive to temperature
	string	central		string	central	
Fall	0.9942	0.9921	string	0.46	2.44	String
Winter	0.9942	0.9941	string	0.48	0.61	String
Spring	0.9942	0.9869	string	0.47	7.03	String
Summer	0.9942	0.9861	string	0.47	8.00	String

Table III Statistical parameters of seasonal time availability index (temperature sensitivity test)

	mean		higher mean value	standard deviation $\times 10^{-3}$		less sensitive to temperature
	string	central		string	central	
Fall	0.9032	0.9073	central	5.83	1.62	central
Winter	0.9034	0.9080	central	5.71	0.99	central
Spring	0.9028	0.9045	central	6.13	4.13	central
Summer	0.9026	0.9018	string	6.32	6.68	string

For a better comparison between the two configurations in different seasons, the statistical results of Figure 4.3 are shown in Table II and III, and corresponding conclusions are presented in the tables based on the mean value and standard deviation of energy and time availability indices. As shown in Table II, in terms of energy availability index, string configuration is dominant over central configuration in terms of higher mean value (higher energy production) and also lower standard deviation (lower sensitivity to temperature change). Intuitively, one can say that the failure of a string inverter blocks the power generation of that string only while the failure of the central inverter blocks the power generation of all strings; this results in higher energy availability index for string configuration.

As Table III shows, in terms of time availability index, in all seasons except the summer, the central configuration is dominant over string configuration in terms of higher mean value and lower standard deviation. Intuitively, one can say that string configuration experiences more failures due to existence of more inverters; however, the high power inputs in summer which cause central inverter encounter a lot of power, dominates the multiplicity of string inverters and results in a more failures in the central inverter during the summer.

From Table II and III, it is perceived that during the summer the performance of string configuration is better than central in terms of both energy and time availability indices. Therefore, as a practical application, one can recommend the string configuration for in areas which have hot weather, while for areas with cold or mild weather more cost/benefit alalysis are required to make a decision.

4.4 **Seasonal Solar Insolation Impact on PV Risk Assessment**

Solar insolation determines the input power of PV inverter, which affects power loss in IGBTs, diodes and capacitors. Thus, a higher insolation will lead to a higher failure rate of the inverter. In the sensitivity study in Figure 4.4, the effect of insolation is quantified by changing the input power of inverter from 0.6 to 1.2 times of the base case input.

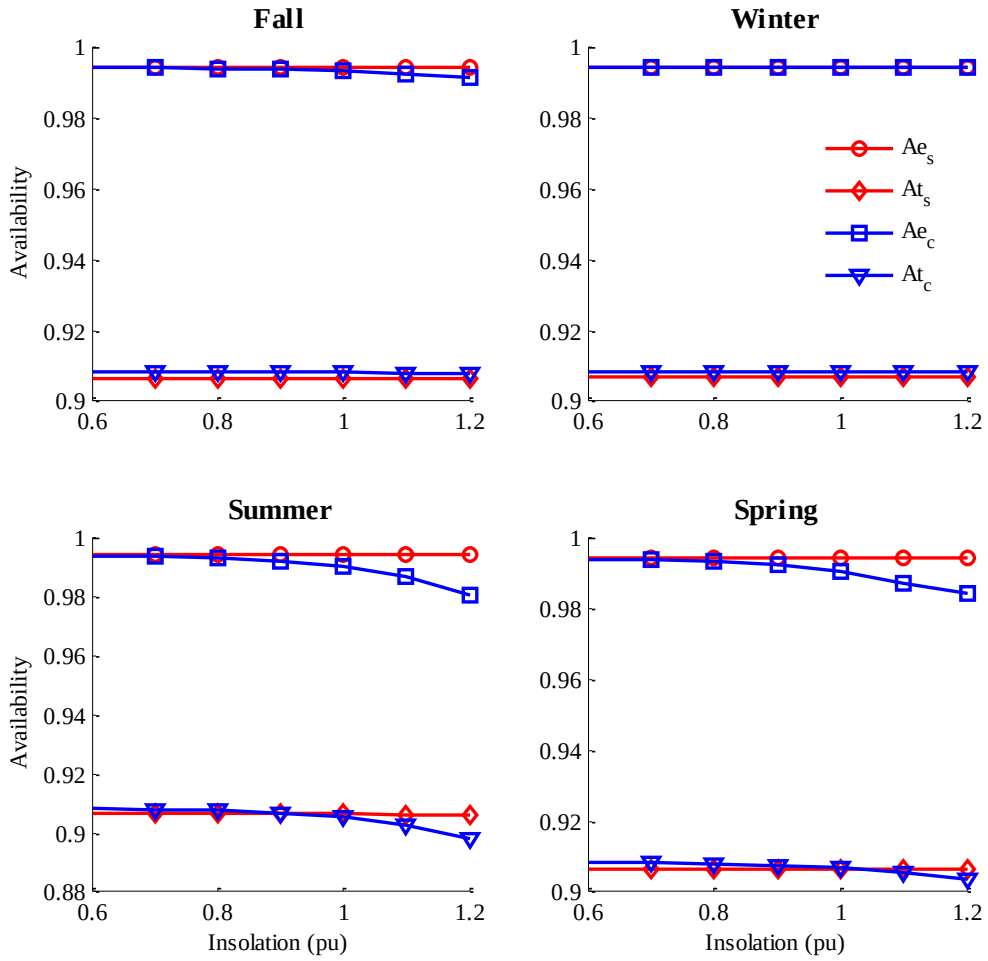

Figure 4.4 Seasonal insolation impact on reliability

It can be observed that from Figure 4.4 that:

(1) A_e of central inverter system is the most vulnerable to insolation variation during summer and spring. It decreases from 99.42% to 98.07% and 90.83% to 89.83%, respectively, due to insolation increase from 0.6 per unit to 1.2.

(2) A_e and A_t of string inverter system are far less impacted by the insolation rise in all seasons due to the system is designed to evenly distribute the input power. As the result, the string inverters experience far less electrical stresses at insolation level above 1 p.u.; hence, the string system has a steady A_e and A_t.

(3) In summer and spring, string system demonstrates better A_e and A_t at insolation level beyond nominal value. This is mainly due to the nonlinear rise of failures of the central inverter system.

Table IV Statistical parameters of seasonal energy availability index (insolation sensitivity test)

	mean		Higher mean value	Standard deviation $\times 10^{-3}$		Less sensitive to insolation
	string	central		string	central	
Fall	0.9941	0.9938	string	1.95e-2	0.89	string
Winter	0.9941	0.9945	central	5.62e-3	3.94e-2	string
Spring	0.9940	0.9923	string	2.99e-2	3.31	string
Summer	0.9940	0.9918	string	3.31e-2	4.35	string

Table V Statistical parameters of seasonal time availability index (insolation sensitivity test)

	mean		Higher mean value	Standard deviation $\times 10^{-3}$		Less sensitive to insolation
	string	central		string	central	
Fall	0.8991	0.9084	central	5.03e-2	0.28	string
Winter	0.8992	0.9086	central	1.29e-2	1.29e-2	-
Spring	0.8990	0.9075	central	0.11	1.57	string
Summer	0.8989	0.9065	central	0.18	3.22	string

For a better comparison between the two configurations with respect to isolation sensitivity, the statistical results of Figure 4.4 are shown in Table IV and V, and corresponding conclusions are presented in the tables based on the mean value and standard deviation of energy and time availability indices. As Table IV shows, in terms of energy availability index, string configuration is dominant over central configuration in terms of higher mean value (higher energy production) and also lower standard deviation (lower sensitivity to temperature change), except for the mean value in winter. This superiority can be traced back to multiplicity of string inverters that a failure of an inverter blocks just the power generation of that specific string. Based on Table V, in

terms of time availability index, string introduces higher sensitivity to insolation and central introduce higher mean value.

4.5 Capacitor ESR Impact on Seasonal Risks of PV Systems

Capacitor equivalent series resistance (ESR) is the resistive part of the capacitor impedance. Electrolytic capacitor, which is commonly used in inverters, tends to have a larger ESR than other types of capacitors. In general, ESR increases as ambient temperature rises which is why electrolytic capacitor is more susceptible to failure. In the sensitivity study in Figure 4.5, the effect of inverter failure is quantified by changing the ESR from 0.2 to 2 times of the base case input.

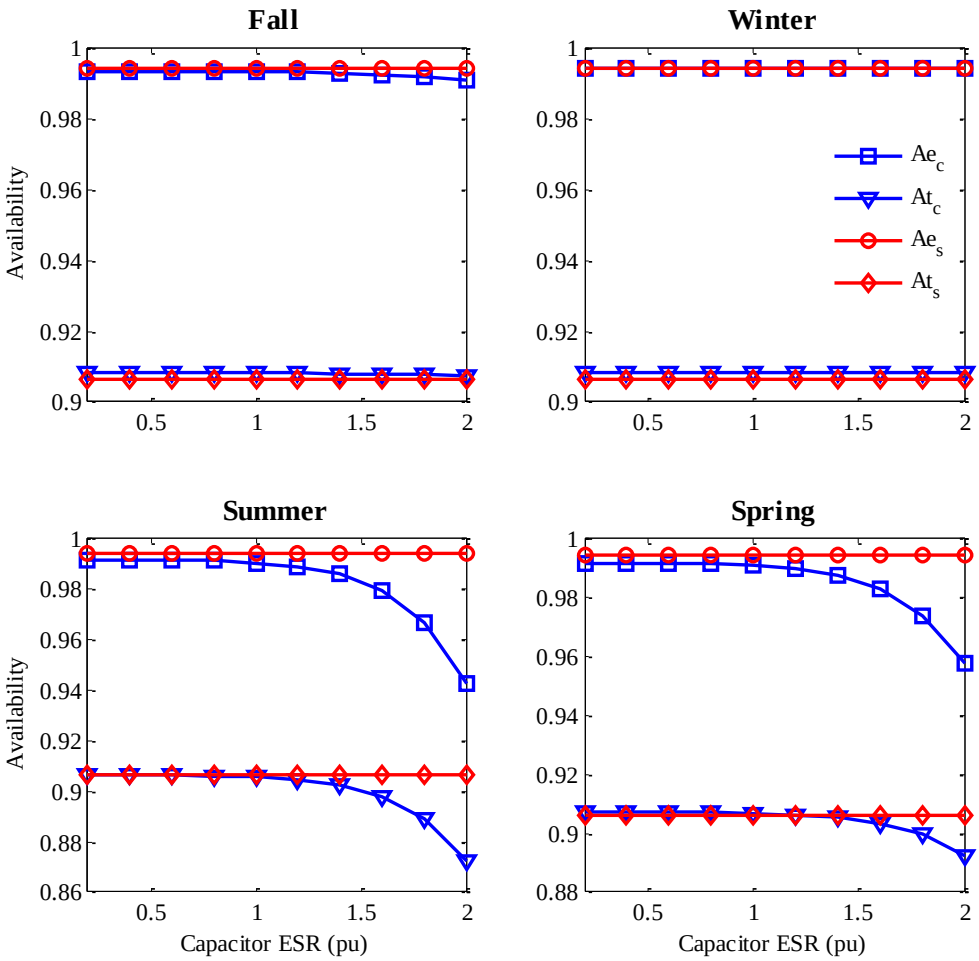

Figure 4.5 Capacitor ESR impact on seasonal reliability

It can be observed from Figure 4.5 that:

(1) String system A_e and A_t are insensitive in all four seasons. The input power of the string system is evenly distributed among the string inverters: $P_o = P_i/N_s$, where P_i is the total input power, P_o is the output power of each string inverter and N_s the number of strings for each phase. According to [4], the RMS ripple current is six times less than the central inverter that results in a significantly lower core temperature T_c. Finally, the lower T_c results in a lower capacitor failure rate and steady A_e and A_t for string system.

(2) Central inverter system, which is equipped with cooling facility, is sensitive to ESR variation in summer and spring. Thus, it is important for system designer to implement an optimally-rated capacitor to ensure system reliability. The above recommendation is especially true for hotter areas.

(3) String system has a better A_e in all four seasons; as of central system has a better A_t when capacitor ESR is equal to or below the nominal value during the summer and spring.

4.6 **Risk as a Function of Number of PV Strings**

A frequently asked question is whether PV system risks can be reduced by a more distributed design [4]? This is investigated by varying the number of strings *n* in the PV array while keeping the total output capacity of the array at 7kW. The risk analysis results are shown in Figure 4.6.

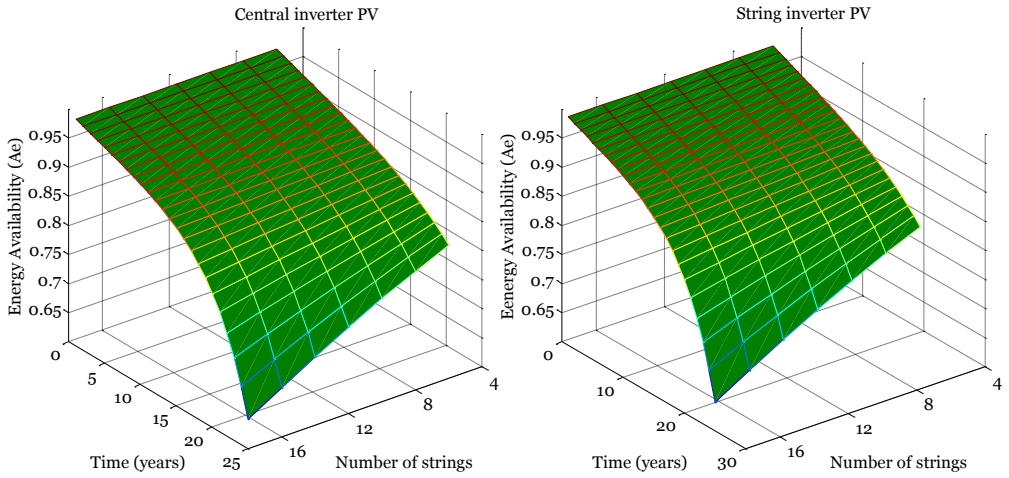

(a) Energy availability (A_e)

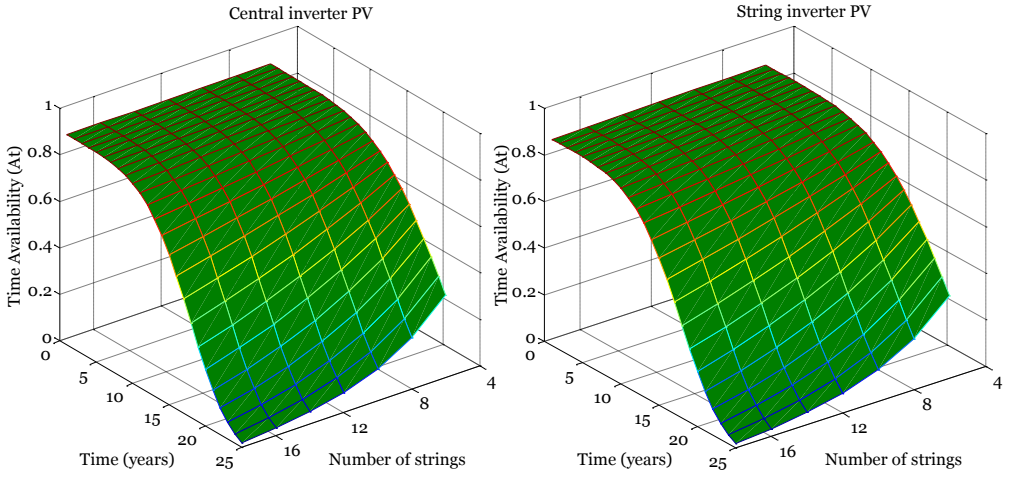

(b) Time availability (A_t)

Figure 4.6 Availability as a function of number of strings

It can be observed from Figure 4.6:

(1) At the beginning of PV system life cycle, both A_e and A_t for the central inverter PV system is insensitive to the increase of n. On the one hand, the failure rate of each string will reduce with the number of panels. On the other hand, more contingencies of strings will occur as n increases. These two opposite effects are almost offset in this case. At the end of PV system life cycle, A_e and A_t drops very quickly with the increase of strings due to aged components in more strings.

(2) For the string inverters, A_e drops slightly for the first ten years with the increase of n. However, the maintenance requirement elevates quickly for the string-inverter PV system when n increases. Taking the first year as an example, when n reaches 16, A_t reduces to 88.57% with an average repair time of 1000 *hrs*/*year* (including the time of partial outages in derated states). Therefore, higher maintenance cost could be a bottleneck that limits the use of the string inverter system, especially when there is a lack of maintenance resource.

4.7 **Effect of Panel Failure Rate on PV Reliability**

The sensitivity analysis results of changing the failure rate of PV panel λ_p are shown in Figure 4.7, from which the following observations can be made:

(1) For both the PV architectures, the sensitivity curve of either A_e or A_t has the same slope with respect to the failure rate of PV panel.

(2) Both the architectures are sensitive to λ_p because each PV string consists of many PV panels in series. In the studied case, there are 96 panels in one string.

(3) A_t is more sensitive to panel failure rate than A_e.

In addition, it may be worthy to point out that the sensitivity curves for the repair time of PV panel are the same as those for the failure rate of PV panel. This is because the availability of PV panel is equal to $\lambda_p r_p/(1+ \lambda_p r_p)$, where the two variables are exchangeable.

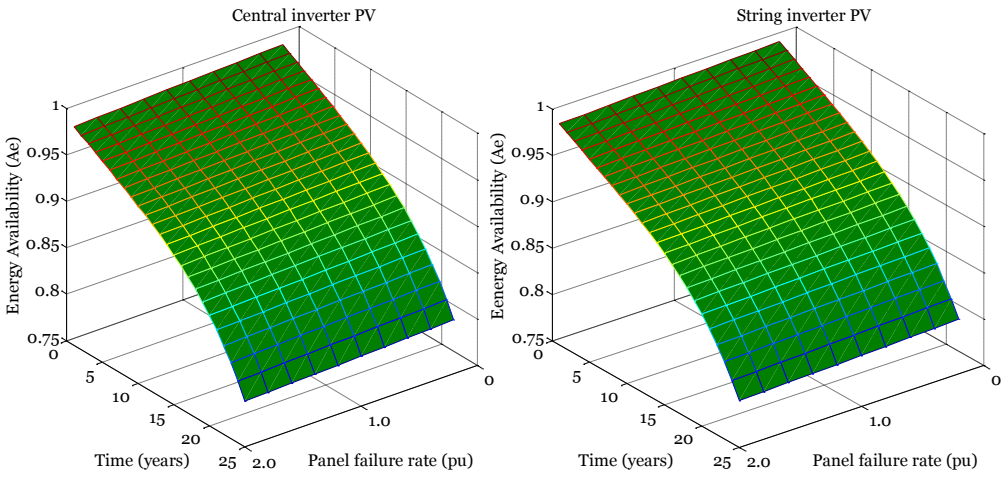

(a) Energy availability (A_e)

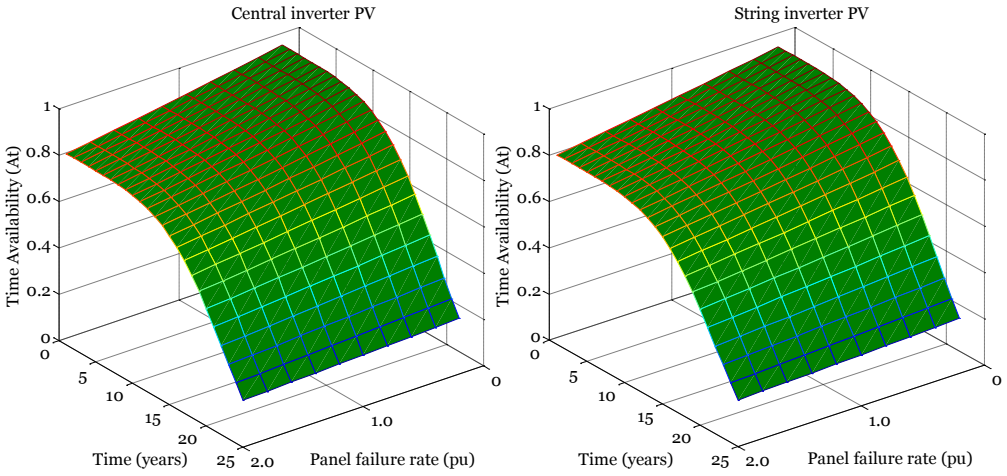

(b) Time availability (A_t)

Figure 4.7 Panel failure rate effect on reliability with degradation

Chapter 5 FUTURE PERSPECTIVE

As PV is becoming a popular source of renewable energy, innovative researchers from the U.S. Defense Advanced Research Projects Agency (DARPA) is trying to create superefficient and compact PV panels that would convert up to 50% solar energy into DC electricity [92]. The heart of this research is to configure PV modules by the new "side-by-side array" design instead of the current "multi-junction stacking" design. Hence, with the promising superefficient PV module development, it is obvious that the average power output of PV plants may increase dramatically into mega-watt or even giga-watt capacity in the future. At a certain point, these Giga-PV plants, which may be interconnected to the grid at the transmission level via feeders at distribution voltage level, will become a reality [93]. On the other hand, these large-scale Giga-PV plants will tend to be installed in remote areas such as the deserts because they take up more land compared with the output-equivalent wind farms or fuel cells. Due to the long distance between deserts and cities, high-voltage transmission lines are usually preferred to efficiently transport the electricity. However, there exist some challenges in terms of power quality, voltage and frequency stability, etc. [94]. The major cause of these challenges comes from the fact that inverters' power electronics often introduce harmonics that may cause grid instability. This problem is amplified as the total ratio of PV generation increases. Thus, proper control strategies must be developed to ensure the grid stability in the future.

One possible research is to study the reliability of transmission integrated with high-voltage PV system, with considerations for power quality, voltage and frequency stability.

Also, more research on PV system degradation due to exposure to harsh environment is needed. This is because as the high-voltage inverters are located in the hot desert, the failure rates of the power electronics switches may be very high.

Chapter 6 CONCLUSION

This thesis reviews the methods for evaluating the reliability of large-scale PV systems and techniques for quantifying the effects of PV interconnection on distribution system reliability. It provides a survey of practical approaches to reliability analysis of PV inverters, PV modules and array, and overall PV power systems. In addition, a comparative study is performed to evaluate the risk performance of central inverter and string inverter grid-tied PV power systems. Major contributions include: 1) risk analysis of seasonal impacts for string and centralized PV systems; and 2) the incorporation of the effect of operational conditions and the aging failure model into PV system risk analysis. The effectiveness of the proposed method has been validated on two real-life 20kW grid-connected PV system designs with central inverter and string inverter structures. The risk performances of the two structures are compared. Seasonal sensitivities of PV system risks to system structure, temperature variation, solar insolation, capacitor equivalent series resistance, number of PV strings, PV panel failure rate and inverter repair time are analyzed. Application of the proposed method to actual large PV systems can provide valuable information to manage PV system risks, to choose better PV system design options, to develop better maintenance strategies, and thus to realize maximum benefit of photovoltaic power.

Chapter 7 REFERENCES

[1] J. Sawin and E. Martinot, "Renewables 2010 global status report," Renewable Energy Policy Network, Tech. Rep. 1, 2010.

[2] P. Lall, "Tutorial: temperature as an input to microelectronics-reliability models," *Reliability, IEEE Transactions On*, vol. 45, pp. 3-9, 1996.

[3] L. Zhang, K. Sun, Y. Xing, L. Feng and H. Ge, "A Modular Grid-Connected Photovoltaic Generation System Based on DC Bus," *Power Electronics, IEEE Transactions On*, vol. 26, pp. 523-531, 2011.

[4] P. Zhang, Y. Wang, W. Xiao and W. Li, "Reliability Evaluation of Grid-Connected Photovoltaic Power Systems," *Sustainable Energy, IEEE Transactions On*, vol. 3, pp. 379-389, 2012.

[5] L. H. Stember, W. R. Huss and M. S. Bridgman, "A Methodology for Photovoltaic System Reliability & Economic Analysis," *Reliability, IEEE Transactions On*, vol. R-31, pp. 296-303, 1982.

[6] S. V. Dhople, A. Davoudi, P. L. Chapman and A. D. Domínguez-García, "Integrating photovoltaic inverter reliability into energy yield estimation with markov models," in *Control and Modeling for Power Electronics (COMPEL), 2010 IEEE 12th Workshop On*, 2010, pp. 1-5.

[7] E. Collins, M. Dvorack, J. Mahn, M. Mundt and M. Quintana, "Reliability and availability analysis of a fielded photovoltaic system," in *Photovoltaic Specialists Conference (PVSC), 2009 34th IEEE*, 2009, pp. 002316-002321.

[8] M. Vazquez and I. Rey-Stolle, "Photovoltaic module reliability model based on field degradation studies," *Progress in Photovoltaics: Research and Applications*, vol. 16, pp. 419-433, August, 2008.

[9] V. Smet, F. Forest, J. Huselstein, F. Richardeau, Z. Khatir, S. Lefebvre and M. Berkani, "Ageing and Failure Modes of IGBT Modules in High-Temperature Power Cycling," *Industrial Electronics, IEEE Transactions On*, vol. 58, pp. 4931-4941, 2011.

[10] G. Petrone, G. Spagnuolo, R. Teodorescu, M. Veerachary and M. Vitelli, "Reliability Issues in Photovoltaic Power Processing Systems," *Industrial Electronics, IEEE Transactions On*, vol. 55, pp. 2569-2580, 2008.

[11] J. Liu and N. Henze, "Reliability consideration of low-power grid-tied inverter for photovoltaic application," in *24th European Photovoltaic Solar Energy Conference and Exhibition*, Hamburg, Germany, 2009, .

[12] A. Pregelj, M. Begovic and A. Rohatgi, "Impact of inverter configuration on PV system reliability and energy production," in *Photovoltaic Specialists Conference, 2002. Conference Record of the Twenty-Ninth IEEE,* 2002, pp. 1388-1391.

[13] E. L. Meyer and E. E. van Dyk, "Assessing the reliability and degradation of photovoltaic module performance parameters," *Reliability, IEEE Transactions On,* vol. 53, pp. 83-92, 2004.

[14] D. Hirschmann, D. Tissen, S. Schroder and R. W. de Doncker, "Reliability prediction for inverters in hybrid electrical vehicles," in *Power Electronics Specialists Conference, 2006. PESC '06. 37th IEEE,* 2006, pp. 1-6.

[15] A. Ristow, M. Begovic, A. Pregelj and A. Rohatgi, "Development of a Methodology for Improving Photovoltaic Inverter Reliability," *Industrial Electronics, IEEE Transactions On,* vol. 55, pp. 2581-2592, 2008.

[16] E. Roman, R. Alonso, P. Ibanez, S. Elorduizapatarietxe and D. Goitia, "Intelligent PV Module for Grid-Connected PV Systems," *Industrial Electronics, IEEE Transactions On,* vol. 53, pp. 1066-1073, 2006.

[17] L. H. Stember, W. R. Huss and M. S. Bridgman, "A Methodology for Photovoltaic System Reliability & Economic Analysis," *Reliability, IEEE Transactions On,* vol. R-31, pp. 296-303, 1982.

[18] J. Liu and N. Henze, "Reliability consideration of low-power grid-tied inverter for photovoltaic application," in *24th European Photovoltaic Solar Energy Conference and Exhibition,* Hamburg, Germany, 2009, pp. 21-25.

[19] E. Hofreiter and A. M. Bazzi, "Single-stage boost inverter reliability in solar photovoltaic applications," in *Power and Energy Conference at Illinois (PECI), 2012 IEEE,* 2012, pp. 1-4.

[20] Z. Shu and P. Jirutitijaroen, "Latin Hypercube Sampling Techniques for Power Systems Reliability Analysis With Renewable Energy Sources," *Power Systems, IEEE Transactions On,* vol. 26, pp. 2066-2073, 2011.

[21] S. V. Dhople, A. Davoudi, A. D. Domínguez-García and P. L. Chapman, "A Unified Approach to Reliability Assessment of Multiphase DC–DC Converters in Photovoltaic Energy Conversion Systems," *Power Electronics, IEEE Transactions On,* vol. 27, pp. 739-751, 2012.

[22] C. Rodriguez and G. A. J. Amaratunga, "Long-Lifetime Power Inverter for Photovoltaic AC Modules," *Industrial Electronics, IEEE Transactions On,* vol. 55, pp. 2593-2601, 2008.

[23] F. Chan and H. Calleja, "Reliability Estimation of Three Single-Phase Topologies in Grid-Connected PV Systems," *Industrial Electronics, IEEE Transactions On,* vol. 58, pp. 2683-2689, 2011.

[24] B. Kroposki, R. Margolis, G. Kuswa, J. Torres, W. Bower, T. Key and D. Ton, "Renewable systems interconnection: Executive summary," NREL Technical Report, Tech. Rep. NREL/TP-581-42292, February. 2008.

[25] J. Bebic and B. Kroposki, "Power system planning: Emerging practices suitable for evaluating the impact of high-penetration photovoltaics." NREL Technical Report, Tech. Rep. NREL/SR-581-42297, February. 2008.

[26] S. V. Dhople and A. D. Dominguez-Garcia, "Estimation of Photovoltaic System Reliability and Performance Metrics," *Power Systems, IEEE Transactions On,* vol. 27, pp. 554-563, 2012.

[27] D. Gaikwad and S. Mehraeen, "Reactive power considerations in reliability analysis of photovoltaic systems," in *Green Technologies Conference, 2012 IEEE,* 2012, pp. 1-6.

[28] I. Bae and J. Kim, "Reliability Evaluation of Customers in a Microgrid," *Power Systems, IEEE Transactions On,* vol. 23, pp. 1416-1422, 2008.

[29] A. K. Basu, S. Chowdhury and S. P. Chowdhury, "Impact of Strategic Deployment of CHP-Based DERs on Microgrid Reliability," *Power Delivery, IEEE Transactions On,* vol. 25, pp. 1697-1705, 2010.

[30] S. B. Patra, J. Mitra and S. J. Ranade, "Microgrid architecture: A reliability constrained approach," in *Power Engineering Society General Meeting, 2005. IEEE,* 2005, pp. 2372-2377 Vol. 3.

[31] J. Mitra, S. B. Patra and S. J. Ranade, "Reliability stipulated microgrid architecture using particle swarm optimization," in *Probabilistic Methods Applied to Power Systems, 2006. PMAPS 2006. International Conference On,* 2006, pp. 1-7.

[32] A. K. Basu, S. P. Chowdhury, S. Chowdhury, D. Ray and P. A. Crossley, "Reliability study of a micro-grid power system," in *Universities Power Engineering Conference, 2008. UPEC 2008. 43rd International,* 2008, pp. 1-4.

[33] A. Kwasinski, "Quantitative Evaluation of DC Microgrids Availability: Effects of System Architecture and Converter Topology Design Choices," *Power Electronics, IEEE Transactions On,* vol. 26, pp. 835-851, 2011.

[34] A. Milo, H. Gaztanaga, I. Etxeberria-Otadui, E. Bilbao and P. Rodriguez, "Optimization of an experimental hybrid microgrid operation: Reliability and economic issues," in *PowerTech, 2009 IEEE Bucharest,* 2009, pp. 1-6.

[35] R. Karki and R. Billinton, "Reliability/cost implications of PV and wind energy utilization in small isolated power systems," *Energy Conversion, IEEE Transactions On,* vol. 16, pp. 368-373, 2001.

[36] Z. Li, Y. Yuan and F. Li, "Evaluating the reliability of islanded microgrid in an emergency mode," in *Universities Power Engineering Conference (UPEC), 2010 45th International,* 2010, pp. 1-5.

[37] J. Park, W. Liang, J. Choi, A. A. El-Keib, M. Shahidehpour and R. Billinton, "A probabilistic reliability evaluation of a power system including solar/photovoltaic cell generator," in *Power & Energy Society General Meeting, 2009. PES '09. IEEE,* 2009, pp. 1-6.

[38] M. Fotuhi-Firuzabad and A. Rajabi-Ghahnavie, "An analytical method to consider DG impacts on distribution system reliability," in *Transmission and Distribution Conference and Exhibition: Asia and Pacific, 2005 IEEE/PES,* 2005, pp. 1-6.

[39] Y. Sun, M. H. J. Bollen and G. W. Ault, "Probabilistic reliability evaluation for distribution systems with DER and microgrids," in *Probabilistic Methods Applied to Power Systems, 2006. PMAPS 2006. International Conference On,* 2006, pp. 1-8.

[40] G. Celli, E. Ghiani, G. G. Soma and F. Pilo, "Active distribution network reliability assessment with a pseudo sequential monte carlo method," in *PowerTech, 2011 IEEE Trondheim,* 2011, pp. 1-8.

[41] W. M. Rohouma, I. M. Molokhia and A. Esuri, "Comparative study of different PV modules configuration reliability," *Desalination,* vol. 209, pp. 122-128, April, 2007.

[42] R. Carbone and A. Tomaselli, "Recent advances on AC PV-modules for grid-connected photovoltaic plants," in *Clean Electrical Power (ICCEP), 2011 International Conference On,* 2011, pp. 124-129.

[43] L. N. Dumas and A. Shumka, "Photovoltaic Module Reliability Improvement through Application Testing and Failure Analysis," *Reliability, IEEE Transactions On,* vol. R-31, pp. 228-234, 1982.

[44] J. H. Wohlgemuth, D. W. Cunningham, A. M. Nguyen and J. Miller, "Long term reliability of PV module," in *20th European Photovoltaic Solar Energy Conference,* Barcelona, Spain, 2005, pp. 1942-1946.

[45] M. Catelani, L. Ciani, L. Cristaldi, M. Faifer, M. Lazzaroni and M. Rossi, "Characterization of photovoltaic panels: The effects of dust," in *Instrumentation and Measurement Technology Conference (I2MTC), 2012 IEEE International,* 2012, pp. 1-4.

[46] S. A. Klein and W. A. Beckman, "Loss-of-load probabilities for stand-alone photovoltaic systems," *Solar Energy,* vol. 39, pp. 499-512, 1987.

[47] R. G. Ross, "Photovoltaic module and array reliability," in *15th IEEE Photovoltaic Specialists' Conference,* Orlando, Florida, 1981, pp. 499-512.

[48] N. K. Gautam and N. D. Kaushika, "Reliability evaluation of solar photovoltaic arrays," *Solar Energy,* vol. 72, pp. 129-141, February, 2002.

[49] F. Chan, H. Calleja and E. Martinez, "Grid connected PV systems: A reliability-based comparison," in *Industrial Electronics, 2006 IEEE International Symposium On*, 2006, pp. 1583-1588.

[50] FIDES Guide 2009, "Reliability methodology for electronics systems," FIDES Group, 2009.

[51] Military Handbook MIL-HDBK-217 Notice 2, *Reliability Prediction of Electronic Equipment.* Washington DC: US Department of Defense, 1995.

[52] Military Handbook MIL-HDBK-217F, *Reliability Prediction of Electronic Equipment.* Washington, DC: US Department of Defense, 1991.

[53] Z. Luo, H. Ahn and M. A. E. Nokali, "A thermal model for insulated gate bipolar transistor module," *Power Electronics, IEEE Transactions On,* vol. 19, pp. 902-907, 2004.

[54] Military Handbook MIL-HDBK-217 Notice 2, *Reliability Prediction of Electronic Equipment.* Washington DC: US Department of Defense, 1995.

[55] S. Clemente, "A simple tool for the selection of IGBTs for motor drives and UPSs," in *Applied Power Electronics Conference and Exposition, 1995. APEC '95. Conference Proceedings 1995., Tenth Annual*, 1995, pp. 755-764 vol.2.

[56] J. J. Nelson, G. Venkataramanan and A. M. El-Refaie, "Fast thermal profiling of power semiconductor devices using Fourier techniques," *Industrial Electronics, IEEE Transactions On,* vol. 53, pp. 521-529, 2006.

[57] L. Wei, R. J. Kerkman, R. A. Lukaszewski, B. P. Brown, N. Gollhardt and B. W. Weiss, "Junction temperature prediction of a multiple-chip IGBT module under DC condition," in *Industry Applications Conference, 2006. 41st IAS Annual Meeting. Conference Record of the 2006 IEEE,* 2006, pp. 754-762.

[58] S. Harb and R. S. Balog, "Reliability of candidate photovoltaic module-integrated-inverter topologies," in *Applied Power Electronics Conference and Exposition (APEC), 2012 Twenty-Seventh Annual IEEE,* 2012, pp. 898-903.

[59] D. Ton and W. Bower. Summary report on the DOE high-tech inverter workshop. US Department of Energy. 2005Available: http://www1.eere.energy.gov/solar/pdfs/ inverter_II_workshop.pdf.

[60] S. G. Parler, "Deriving life multipliers for electrolytic capacitors," *IEEE Power Electronic Soc. Newsletter,* vol. 16, pp. 11-12, 2004.

[61] A. Albertini, M. G. Masi, G. Mazzanti, L. Peretto and R. Tinarelli, "Toward a BITE for Real-Time Life Estimation of Capacitors Subjected to Thermal Stress," *Instrumentation and Measurement, IEEE Transactions On,* vol. 60, pp. 1674-1681, 2011.

[62] G. Graditi and G. Adinolfi, "Temperature influence on photovoltaic power optimizer components reliability," in *Power Electronics, Electrical Drives, Automation and Motion (SPEEDAM), 2012 International Symposium On,* 2012, pp. 1113-1118.

[63] Anonymous *Application Guide, Aluminum Electrolytic Capacitors.* Liberty, SC: Cornell Dubilier, 2003.

[64] M. Rashid, "Power Electronics Handbook," pp. 1409, 2010.

[65] D. Hirschmann, D. Tissen, S. Schroder and R. W. De Doncker, "Inverter design for hybrid electrical vehicles considering mission profiles," in *Vehicle Power and Propulsion, 2005 IEEE Conference,* 2005, pp. 6 pp.

[66] P. D. Evans and R. J. Hill-Cottingham, "DC link current in PWM inverters," *Electric Power Applications, IEE Proceedings B,* vol. 133, pp. 217-224, 1986.

[67] A. Mariscotti, "Analysis of the DC-link current spectrum in voltage source inverters," *Circuits and Systems I: Fundamental Theory and Applications, IEEE Transactions On,* vol. 49, pp. 484-491, 2002.

[68] J. W. Kolar and S. D. Round, "Analytical calculation of the RMS current stress on the DC-link capacitor of voltage-PWM converter systems," *Electric Power Applications, IEE Proceedings -,* vol. 153, pp. 535-543, 2006.

[69] A. D. Dominguez-Garcia and P. T. Krein, "Integrating reliability into the design of fault-tolerant power electronics systems," in *Power Electronics Specialists Conference, 2008. PESC 2008. IEEE,* 2008, pp. 2665-2671.

[70] E. Koutroulis and F. Blaabjerg, "Design Optimization of Transformerless Grid-Connected PV Inverters Including Reliability," *Power Electronics, IEEE Transactions On,* vol. 28, pp. 325-335, 2013.

[71] G. J. Anders and A. M. Leite da Silva, "Cost related reliability measures for power system equipment," *Power Systems, IEEE Transactions On,* vol. 15, pp. 654-660, 2000.

[72] A. B. Maish, C. Atcitty, S. Hester, D. Greenberg, D. Osborn, D. Collier and M. Brine, "Photovoltaic system reliability," in *Photovoltaic Specialists Conference, 1997., Conference Record of the Twenty-Sixth IEEE,* 1997, pp. 1049-1054.

[73] L. N. Kishore and E. Fernandez, "Reliability well-being assessment of PV-wind hybrid system using monte carlo simulation," in *Emerging Trends in Electrical and Computer Technology (ICETECT), 2011 International Conference On,* 2011, pp. 63-68.

[74] M. M. Ghahderijani, S. M. Barakati and S. Tavakoli, "Reliability evaluation of stand-alone hybrid microgrid using sequential monte carlo simulation," in *Renewable Energy and Distributed Generation (ICREDG), 2012 Second Iranian Conference On,* 2012, pp. 33-38.

[75] R. Billinton, Hua Chen and R. Ghajar, "A sequential simulation technique for adequacy evaluation of generating systems including wind energy," *Energy Conversion, IEEE Transactions On,* vol. 11, pp. 728-734, 1996.

[76] F. Vallee, J. Lobry and O. Deblecker, "Impact of the Wind Geographical Correlation Level for Reliability Studies," *Power Systems, IEEE Transactions On,* vol. 22, pp. 2232-2239, 2007.

[77] A. M. Leite da Silva, L. A. Da Fonseca Manso, J. C. De Oliveira Mello and R. Billinton, "Pseudo-chronological simulation for composite reliability analysis with time varying loads," *Power Systems, IEEE Transactions On,* vol. 15, pp. 73-80, 2000.

[78] P. M. Subcommittee, "IEEE Reliability Test System," *Power Apparatus and Systems, IEEE Transactions On,* vol. PAS-98, pp. 2047-2054, 1979.

[79] Mei-Chen Hsueh, T. K. Tsai and R. K. Iyer, "Fault injection techniques and tools," *Computer,* vol. 30, pp. 75-82, 1997.

[80] R. Natella, D. Cotroneo, J. Duraes and H. Madeira, "On Fault Representativeness of Software Fault Injection," *Software Engineering, IEEE Transactions On,* vol. PP, pp. 1-1, 2012.

[81] W. Xiao and P. Zhang, "Photovoltaic voltage regulation using affine parameterization," *Green Energy,* In press.

[82] C. L. Masters, "Voltage rise: the big issue when connecting embedded generation to long 11 kV overhead lines," *Power Engineering Journal,* vol. 16, pp. 5-12, 2002.

[83] E. Lakervi, E. J. Holmes and Institution of Electrical Engineers, *Electricity Distribution Network Design.* London: P. Peregrinus on behalf of the Institution of Electrical Engineers, 1995.

[84] Y. Ueda, K. Kurokawa, T. Tanabe, K. Kitamura and H. Sugihara, "Analysis Results of Output Power Loss Due to the Grid Voltage Rise in Grid-Connected Photovoltaic Power Generation Systems," *Industrial Electronics, IEEE Transactions On,* vol. 55, pp. 2744-2751, 2008.

[85] Y. Wang, P. Zhang and W. Li, "Online overvoltage prevention control of photovoltaic generators in microgrids," *IEEE Trans. of Smart Grid,* In press.

[86] R. Tonkoski, L. A. C. Lopes and T. H. M. El-Fouly, "Coordinated Active Power Curtailment of Grid Connected PV Inverters for Overvoltage Prevention," *Sustainable Energy, IEEE Transactions On,* vol. 2, pp. 139-147, 2011.

[87] P. Zhang, H. Xue and R. Yang, "Shifting Window Average Method for Accurate Frequency Measurement in Power Systems," *Power Delivery, IEEE Transactions On,* vol. 26, pp. 2887-2889, 2011.

[88] B. Gudimetla, F. Katiraei, J. R. Aguero, J. H. R. Enslin and H. Alatrash, "Integration of micro-scale photovoltaic distributed generation on power distribution systems: Dynamic analyses," in *Transmission and Distribution Conference and Exposition (T&D), 2012 IEEE PES*, 2012, pp. 1-7.

[89] S. Cha, D. Jeon, I. Bae, I. Lee and J. Kim, "Reliability evaluation of distribution system connected photovoltaic generation considering weather effects," in *Probabilistic Methods Applied to Power Systems, 2004 International Conference On,* 2004, pp. 451-456.

[90] Gwang-Seob Kim and K. Lee, "Fault diagnosis and fault-tolerant control of a dc-link voltage sensor for PV inverters," in *Power Electronics and Motion Control Conference (IPEMC), 2012 7th International,* 2012, pp. 1408-1412.

[91] S. Sridhar, A. Hahn and M. Govindarasu, "Cyber attack-resilient control for smart grid," in *Innovative Smart Grid Technologies (ISGT), 2012 IEEE PES,* 2012, pp. 1-3.

[92] R. Stevenson, "Tapping the Power of 100 Suns," *IEEE Spectrum Magazine- Green Tech - Solar,* 2012.

[93] R. A. Walling and K. Clark, "Grid support functions implemented in utility-scale PV systems," in *Transmission and Distribution Conference and Exposition, 2010 IEEE PES,* 2010, pp. 1-5.

[94] Y. Weidong, Z. Xia and X. Feng, "Impacts of large scale and high voltage level photovoltaic penetration on the security and stability of power system," in *Power and Energy Engineering Conference (APPEEC), 2010 Asia-Pacific,* 2010, pp. 1-5.

APPENDIX

Reliability Parameters for the Central Configuration PV System Connected to BC Hydro Grid

TABLE A-I
PARAMETERS FOR RELIABILITY ANALYSIS OF BASE CASE

IGBT & Diode				
T_a(℃)	μ	$cos\varphi$	V_t(V)	f(kHz)
25	0.8	0.95	480	20
P_{add}(W)	θ_a(℃/W)	V_{1o}(V)	a_1	b_1
11	0.11	0.9654	0.1642	0.6468
k	z	h	r	$V_{r,\ IGBT}$ (V)
1.6783	0.0181	0.0040	1.3444	480
θ_{11}(℃/W)	θ_{12}(℃/W)	θ_{21}(℃/W)	θ_{22}(℃/W)	r_{Di}(days)
0.640	0.250	0.300	0.830	20
λ_{0TH}	$\Pi_{Induced}$	Π_{PM}	$\Pi_{Process}$	r_{Si}(days)
0.3021	2.0	1.7	4.0	20
k_{goff}	k_{gon}	$V_{r,\ diode}$(V)	t_a(ns)	t_b(ns)
1.0	1.5	600	25.9	54.1
V_{2o}(V)	a_2	b_2	I_{rr}(A)	
0.711	0.136	0.395	10	
λ_b	π_E	π_C	π_Q	
0.005	6.0	1.0	2.4	
Capacitor				
L_b(hours)	T_{max}(℃)	R_s(Ω)	θ_c(℃/W)	r_C(days)
20000	95	0.02	15.6	10

PV array						
$\lambda_{P,i}$	$r_{P,i}$	λ_F	r_F	d	α	β
1.1416	48	5.7078	10	0.5%	26.99	5.83

DC disconnect and AC subpanel			
λ_{DC}	r_{DC}	λ_{AC}	r_{AC}
0.05	16	0.01	10

Note: The unit for the failure rates is $1/(10^6 hrs)$ and repair time is *hrs*.

Reliability Parameters for the String Configuration PV System Connected to BC Hydro Grid

TABLE A-II
PARAMETERS FOR RELIABILITY ANALYSIS OF BASE CASE (STRING)

IGBT & Diode				
T_a(℃)	μ	$cos\varphi$	V_t(V)	f(kHz)
25	0.8	0.95	480	20
P_{add}(W)	θ_a(℃/W)	V_{1o}(V)	a_1	b_1
11	0.11	0.9654	0.1642	0.6468
k	z	h	r	$V_{r,\ IGBT}$ (V)
1.6783	0.0181	0.0040	1.3444	480
θ_{11}(℃/W)	θ_{12}(℃/W)	θ_{21}(℃/W)	θ_{22}(℃/W)	r_{Di}(days)
0.640	0.250	0.300	0.830	20
λ_{0TH}	$\Pi_{Induced}$	Π_{PM}	$\Pi_{Process}$	r_{Si}(days)
0.3021	2.0	1.7	4.0	20
k_{goff}	k_{gon}	$V_{r,\ diode}$(V)	t_a(ns)	t_b(ns)
1.0	1.5	600	25.9	54.1
V_{2o}(V)	a_2	b_2	I_{rr}(A)	
0.711	0.136	0.395	10	

λ_b	π_E	π_C	π_Q
0.005	6.0	1.0	2.4

Capacitor

L_b(hours)	T_{max}(°C)	R_s(Ω)	θ_c(°C/W)	r_C(days)
20000	95	0.2	4.52	10

PV array

$\lambda_{P,i}$	$r_{P,i}$	λ_F	r_F	d	α	β
1.1416	48	5.7078	10	0.5%	26.99	5.83

DC disconnect and AC subpanel

λ_{DC}	r_{DC}	λ_{AC}	r_{AC}
0.05	16	0.01	10

Note: The unit for the failure rates is $1/(10^6 hrs)$ and repair time is *hrs*.